2018 25th Congress of International Federation for Heat Treatment and Surface Engineering

11-14 September 2018 | Xi`an China

PROCEEDINGS

Organized by Chinese Heat Treatment Society（CHTS）

25th IFHTSE CONGRESS PROCEEDINGS

11-14 September 2018

Xi'an China

Chinese Heat Treatment Society

Tel：+86（0）10 6292 0613 • Email：chts@chts.org.cn • Web:www.chts.org.cn

Add: 18 Xueqing Rd.,Beijing,China

Non-ferrous Metals, Cu, Al, Mg, Ti alloy, and etc

Heat Treatment and Surface Engineering in Energy Industry

Improvement of mechanical biocompatibility of titanium alloys for biomedical applications by deformation-induced phase transformation

Mitsuo Niinomi[1,2,3,4,5]

(1. Tohoku University; 2. Specially Appointed Professor, Graduate School of Engineering, Osaka University; 3. Graduate School of Science and Engineering, Meido University; 4. Institute for Materials Research, Tohoku University; 5. Institute of Materials and Systems for Sustainability, Nagoya University)

Abstract: The main popular metallic biomaterials are stainless steel, Co-Cr-Mo alloys, and titanium (Ti) and its alloys. Ti alloys are the most reliable metallic biomaterials among them. Mechanical biocompatibilities including Young's modulus, strength and ductility, fatigue strength, fracture toughness, and wear resistance are important properties for metallic biomaterials as well as biological biocompatibilities. Mechanical biocompatibility of Ti alloys for biomedical applications can be improved by melting process, wrought process, heat treatment, thermomechanical treatment, and surface treatment. After fabricating implant devices using Ti alloys, improving their mechanical biocompatibilities is difficult by adopting above mentioned methods with maintaining the structure and functionality of implant devices. In that case, deformation-induced transformation is expected to be effectively applied to improve mechanical biocompatibilities of implant devices made of Ti alloys.

The deformation-induced transformation occurs in Ti alloys comprising metastable β-phase. According to the stability of the β-phase, it transforms to α' martensite, α" martensite, ω-phase, and twins. Then, the deformation-induced martensite transformation improves fracture toughness and crack propagation resistance of (α+β)-type Ti alloys such as Ti-6Al-4V for biomedical applications. The deformation-induced twinning improves both strength and ductility of metastable β-type Ti alloys with the deformation-induced martensite or ω-phase transformation; this phenomenon is called as twinning induced plasticity (TWIP). Young's moduli of some metastable β-type Ti alloys are increased by deformation because the deformation-induced ω-phase transformation occurs; this phenomenon is effective to keep the bending shape of the rod for the spinal fixation device. Ti alloys showing this kind of phenomenon are referred to as Young's modulus changeable Ti alloys. The addition of a large amount of oxygen improves the fatigue strength of a certain metastable β-type Ti alloy by both solid-solution strengthening due to solved oxygen and microstructural refinement due to deformation-induced martensite transformation. The example of this phenomenon is shown in Fig.1[1] ng the S-N curves of the metastable β-type Ti alloy, Ti-29Nb-13Ta-4.6Zr (referred to as TNTZ), with an oxygen content of from 0 to 0.7mass% subjected to solution treatment (ST). The fatigue strength of TNTZ increases with increasing the oxygen content and reaches to the middle level of the fatigue limit of Ti-6Al-4V ELI. Fig.2[1] shows the transmission electron microscopy (TEM) micrographs including BF images, selected area electron diffraction (SAED) patterns and dark field (DF) images (DF image was acquired using the diffraction spot marked by the circle in its corresponding SAED pattern) of TNTZ with oxygen contents of 0.1, 0.5, and 0.7mass% after cyclic loading at 10^5 cycles (areas containing plate-like structures were selected to be detected). The width of the deformation-induced α" martensite decreases with increasing the content of oxygen indicating microstructural refinement.

The improvement of mechanical biocompatibilities such as Young's modulus, balance of strength and ductility, and fatigue strength of Ti alloys with metastable β-phase for biomedical applications by the deformation-induced phase transformation will be discussed in this talk.

Keywords: titanium alloys, metastable β-phase, mechanical biocompatibility, deformation-induced phase transformation

Reference:

[1] H. Liu, M. Niinomi, M. Nakai, S. Obara and H. Fujii: Mater. Sci. Eng. A, 704(2017), pp. 10-17.

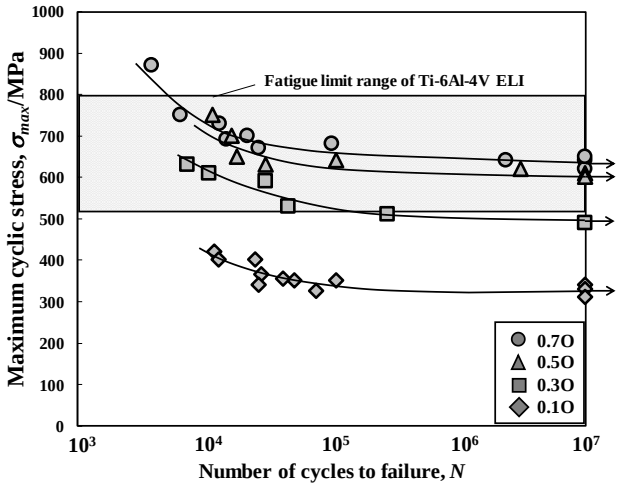

Fig.1 S-N curves of TNTZ with oxygen contents of 0.1, 0.3, 0.5, and 0.7mass%O (referred to as 0.1O, 0.3O, 0.5O, and 0.7O, respectively) with fatigue limit range of Ti-6Al-4V ELI

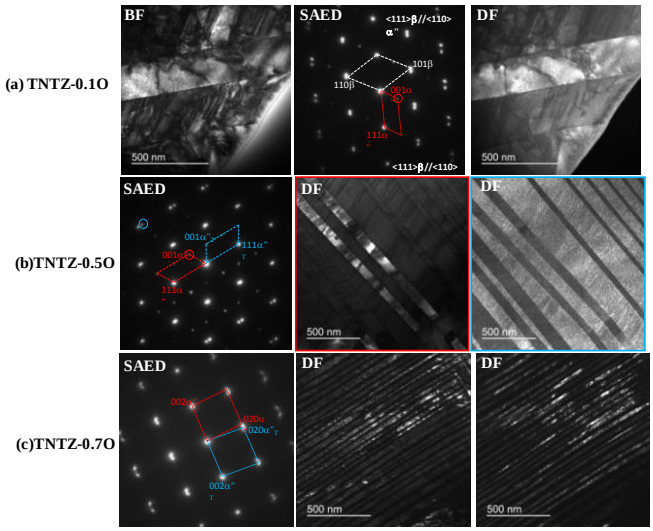

Fig.2 TEM micrographs including BF images, selected area electron diffraction (SAED) patterns and dark field (DF) images (DF image was acquired using the diffraction spot marked by the circle in its corresponding SAED pattern) of TNTZ with (a) 0.1 (TNTZ-0.1), (b) 0.5 (TNTZ-0.5O), and (c) 0.7 (TNTZ-0.7O) mass%O after cyclic loading at 10^5 cycles

Effect of high temperature strain rate and subsequent annealing on recrystallization behavior of Ti-55531 alloy

Hui Shao, Lulu Cai
(Xi'an University of Technology)
904629056@qq.com

Abstract: Ti-55531 (Ti-5Al-5Mo-5V-3Cr-1Zr) is a relatively new near β titanium alloy. Owing to high strength and excellent fracture toughness, good hardenability, it is used to fabricate the large load-bearing components in aerospace industry. The static recrystallization plays an important role in microstructure evolution and mechanical property after deformation. Ti55531 alloy is very sensitive to deformation parameters, which will affect the size and morphology of recrystallization phase by the subsequent heat treatment process.

The Ti55531 alloy with an equiaxed structure was used in this experiment, consisting of predominant equiaxed α phase and residual β phase. In this work, the α/β transus temperature has been measured as 840 ℃ by OM method. The cylindrical samples with 15 mm in height and 10 mm in diameter. The hot compression tests with different strain rates (0.01, 0.1 and 1 s^{-1}) were carried out using Gleeble 3800 at 900 ℃. The tests were carried out in a vacuum environment in order to prevent the oxidation in the high temperature. After compression deformation, the samples were cut axially to observe the microstructure by OM, SEM. In addition, the annealing at 750 ℃ for 5 min were conducted in the furnace. The samples were immediately water-cooled so as to reserve compression deformation and heat treatment microstructures after each experiment. The size and orientation of phases were observed using an EBSD system in scanning electron microscope (Carl Zeiss Microscopy GmbH). The grain boundaries with the misorientation angle between 2 °and 15 °were defined as low-angle boundaries (LABs). The high-angle boundaries (HABs) were those of misorientation angle above 15 °. In order to further observation the dislocation morphology, a thin TEM foil was prepared in a twin-jet electro-polishing unit with an electrolyte of 6% perchloric acid, 60% methanol and 34% n-butyl alcohol at ~25 ℃.

In conclusion, the flow stress increases with the increase of the strain rate. β phases are apparently elongated at low strain rate, which lead to subgrains development at β phase boundaries. With the further increase of strain rate, a large number of α phases retained at β phase boundaries were observed. The density of defects including dislocations and substructures increases with increasing the strain rate. During the subsequent heat treatment, a large amount of dislocations provides the force of static recrystallization of α and β phases. The HAGBs content is the highest and the recrystallized grains are the most at strain rate is 0.1 s^{-1}. The recrystallization occurs more completely in β phase than in α phase. Furthermore, combined with EBSD and TEM, the evolution mechanism of recrystallized structure was analyzed and discussed.

Keywords: strain rate, heat treatment, recrystallization, Ti-55531

Effect of Ni content on microstructure and characterization of Cu-Ni-Sn alloys

Xiaochao Wang[1], Zhen Li[1], Sanming Du[1], Zhenghai Yang[1], Yongzhen Zhang[1], Jingbo Wang[2]
(1. National United Engineering Laboratory for Advanced Bearing Tribology,
Henan University of Science and Technology;
2. State Key Laboratory of Solid Lubrication, Lanzhou Institute of Chemical Physics,
Chinese Academy of Sciences)
dsming@haust.edu.cn

Abstract: The Cu-Ni-Sn alloys attracted wide interest in electronic and mechanical industries because of high strength, good thermal and electrical conductivity, and so on. So, many researchers focused attention on the investigations of the mechanical properties and microstructural evolution of Cu-Ni-Sn alloys with aging treatment. However, the studies on the effect of Ni content on microstructure and characterization of Cu-Ni-Sn alloys prepared by powder metallurgy technique have been rarely reported yet. Therefore, the aim of the present work is to investigate the effect of Ni content on hardness, yield strength, microstructure and morphology of Cu-*x*Ni-5Sn (wt%) alloys and discuss the relationship between the microstructure and mechanical properties of Cu-*x*Ni-5Sn (wt%) alloys. In this paper, Cu-*x*Ni-5Sn (wt%) alloys with different Ni contents were prepared by a powder metallurgy method to avoid component segregation. Commercially available powders of Cu, Ni and Sn were weighed according to the pre-designed weight ratios and then the metal powders were mechanically mixed using a three-dimensional vibration blender for 4-5 h. The mixed metal powders were firstly cool pressed and then sintered at 885 ℃ for about 65 min in the tube furnace under hydrogen atmosphere, subsequently aging treatment was performed at 400 ℃ for about 4 h in the tube furnace under hydrogen atmosphere.

The effect of Ni content on hardness and yield strength of Cu-*x*Ni-5Sn alloys before and after aging treatment were investigated. The microstructure, composition and morphology of Cu-xNi-5Sn alloys were observed by X-ray diffraction (XRD), scanning electron microscopy (SEM) with energy dispersive spectroscopy (EDS) and cold field emission scanning electron microscope (FESEM), respectively. Results indicate that hardness and yield strength firstly increase and then decrease with the increase of Ni content and reach up to a maximum when Ni content is 12.5wt%. The XRD patterns show that the phase constituents of the Cu-*x*Ni-5Sn alloys before and after aging treatment are not obvious different and basically similar, and the phase constituents are mainly composed of Cu/Cu solid solution and CuNi2Sn. The SEM micrographs show that the lamellar precipitated phases of Cu12.5Ni-5Sn alloys after aging treatment increase significantly and the formation of lamellar precipitates in the matrix generates the sandwich structures. The needle-like phase in the grain is found in Cu-12.5Ni-5Sn alloys after aging treatment. Furthermore, the grain boundary and intragranular precipitates are rich in both Ni and Sn phase. The lamellar precipitate of the sandwich structure of the alloys after aging treatment is slightly different with the increasing of Ni content. The formation of the inerratic and suitable lamellae of sandwich structure and needle-like phase can be responsible for the good mechanical properties of the Cu-12.5Ni-5Sn alloy after aging treatment.

Keywords: Cu-Ni-Sn alloys, mechanical properties, precipitate, microstructure

Designing Mg alloy with high strength and ductility through optimizing microstructure and texture

Yuzhou Du[1,2], Jiqiang Qi[1,2], Bailing Jiang[1,2], Yanfeng Ge[1,2], Mingyi Zheng[3],
(1. School of Materials Science and Engineering, Xi'an University of Technology;
2. Shaanxi Province Engineering Research Center for Magnesium Alloys, Xi'an University of Technology;
3. School of Materials Science and Engineering, Harbin Institute of Technology)
duyuzhou@xaut.edu.cn

Abstract: A Mg-Zn based alloy with high strength and ductility was designed through microstructural control. Firstly, the texture evolution of Mg-Zn binary alloy during recrystallization was investigated. It was found that dynamic recrystallization weakened the texture intensity by contrast to the deformed region. The fine DRXed region exhibited a weaker texture compared with the coarse DRXed region, which was related to the suppressed grain boundaries migration due to second phase at grain boundaries. Additionally, a remarkable grain-size driven textural transition from <10.0> - <11.0> texture to <11.0> texture for the DRXed grains were detected. The recrystallized grains with small grain size showed a fiber texture distributing homogeneously between <10.0> and <11.0>, while <11.0> fiber texture was predominant for the large recrystallized grains. It is suggested that grains of <11.0> fiber texture grow faster than grains of other orientations, which is ascribed to a larger misorientation between <11.0> fiber texture grains and their neighboring matrix than that between other grains and the matrix. Based on the investigation, it was found that a homogeneous distribution of stable precipitates around grain boundaries might be an ideal microstructure for mechanical properties improvement. Then a rolled Mg-Zn-Ca-La alloy with high strength and ductility was fabricated. The detailed microstructure and mechanical properties were investigated.

Keywords: Mg-Zn alloy, microstructure, texture, recrystallization

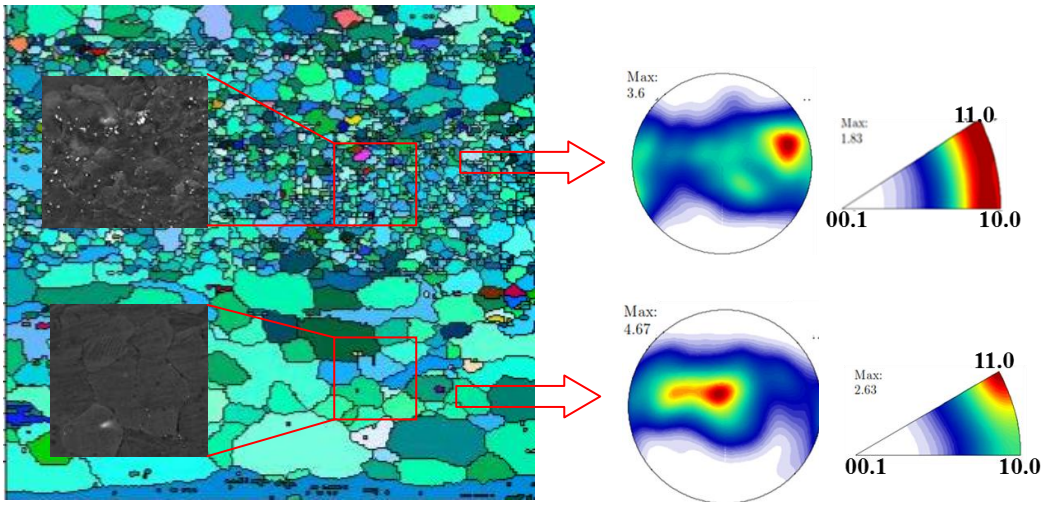

Fig.1

Effect of heat treatment on microstructure and mechanical properties of Al-4.5Cu-1Mg-0.5Mn(-*x*Er) alloys

Xiaoran Huo, Qingyan Zhu, Xuegang Wang, Feng Li, Lijia Chen
(Shenyang University of Technology)
chenlj-sut@163.com

Abstract: Aluminum alloys have such characteristics as low density, high specific strength and rigidity, and have found a wide application in aeronautical and automotive industries. To extend the application field of aluminum alloys, some measures, which can improve the microstructure, strength and plasticity of aluminum alloys, have to be taken. Usually, the rare earth elements are recognized as one of the most effective elements available to improve both microstructure and property of aluminum alloys, rare earth elements can effectively refine the grain size of aluminum alloys, thereby exerting their metamorphism. In addition to metamorphism, strengthening, and purification of impurities in aluminum alloys, rare earth elements can often improve the casting process, the high temperature performance and the optical and electrical properties of aluminum alloys. And thus, research concerning the action of rare earth elements in aluminum alloys is of both important theoretical referring value and practical directing significance for developing new aluminum alloys with high strength and ductility.

As a representative of high-strength extruded aluminum alloys, Al-Cu-Mg extruded aluminum alloys have excellent comprehensive properties, however, with the increasing number of applications of Al-Cu-Mg extruded aluminum alloys and the expanding range of applications, the demand for their comprehensive performances also have increased. In this investigation, the Al-4.5Cu-1Mg-0.5Mn alloy was chosed as the master alloy. Through adding Er as well as melting, casting and hot extrusion, the Al-4.5Cu-1Mg-0.5Mn(-*x*Er) alloys with Er have been fabricated. Analyzed the effect of Er on the combination properties of Al-4.5Cu-1Mg-0.5Mn(-*x*Er) alloys through tensile tests, metallographic and microstructure, in order to provide theoretical basis for the engineering application of this kind of extruded aluminum alloys .

The experimental results show that the addition of rare earth element Er can refine the grains of the extruded Al-4.5Cu-1Mg-0.5Mn alloys with both as-extruded and solid solution plus aging states to some extent. When 0.3% rare earth element Er are added into Al4.5Cu-1Mg-0.5Mn alloys, the microstructure of extruded Al-4.5Cu-1Mg-0.5Mn-0.3Er alloys will be obviously refined, and the T6 state of this alloys have more uniform structures. When 0.5% rare earth element Er are added into Al-4.5Cu-1Mg-0.5Mn alloys, dendrite tissues have appeared in the microstructure of extruded Al-4.5Cu-1Mg-0.5Mn-0.5Er alloys , and the grain sizes of the T6 state of this alloy have been further refined, meanwhile the grain sizes of this alloy treated by solid solution for 3 h plus aging for 12 h are the smallest. Solid solution plus aging treatment can effectively improve the tensile strength, yield strength and elongation at break of Al-4.5Cu-1Mg-0.5Mn alloys, meanwhile the tensile strength and yield strength of the extruded Al-4.5Cu-1Mg-0.5Mn-0.3Er alloys treated with solid solution for 3 h plus aging for 12 h are the highest. Under the same heat treatment conditions, the tensile fracture of Al-4.5Cu-1Mg-0.5Mn-0.3Er alloys with rare earth element Er at room temperature are easy to appear ductile fracture morphology than Al-4.5Cu1Mg-0.5Mn alloys and Al-4.5Cu-1Mg-0.5Mn-0.5Er alloys, at the same time, dimples in fracture surface morphology of Al-4.5 Cu-1Mg-0.5Mn-0.3Er alloys are smaller , deeper and the number of tear edges around dimples are more.

Keywords: aluminum alloy, microstructure, rare earth element Er, solid solution plus aging treatment

Influence of solution and aging treatment on microstructure and mechanical properties of extruded Al-7Zn-2Mg-1.5Cu-0.1Zr(-0.2Sc) alloy

Qingyan Zhu, Xiaoran Huo, Lijia Chen
(Shenyang University of Technology)
chenlj-sut@163.com

Abstract: As a typical age-hardenable alloy, Al-Zn-Mg-Cu series alloys processed in the form of plates, extrusions or forgings, are widely used in the structure of the aircraft and automobile parts because of their high specific strength and good ductility. The improvement of alloy performance is anticipated by main element content design, micro alloying and heat treatment. In this paper, two kinds of Al-Zn-Mg-Cu-Zr alloys with and without Sc additions were applied for comparative research. The nominal chemical compositions of the two alloys are described as Al-7Zn-2Mg-1.5Cu-0.1Zr(-0.2Sc) (wt%). The experimental alloy ingots were extruded into bars after homogenization treatment at 470 ℃ for 24 h, the extrusion temperature is 450 ℃, the squeeze ratio is about 40. The alloy bars were subjected to solution treatment at 475 ℃ for 1 h, followed by water quenching, and then aged at 120 ℃ for various times from 20 h to 56 h. The microstructure and mechanical properties of the novel Al-Zn-Mg-Cu-Zr(-Sc) alloy under different aging time were investigated by means of transition electron microscopy (TEM), hardness measurement and tensile experiment, the fracture mode of alloys was observed by scanning electron microscopy (SEM), to provide reliable theoretical basis for the engineering application of this kind of aluminum alloy.

The results of mechanical properties tests indicate that the aging strengthen tendency of Al-Zn-Mg-Cu-Zr(-Sc) alloys exhibit similar double peaks feature on the hardness and strength of the studied alloys during the whole of aging period. And the Brinell hardness, ultimate tensile strength (UTS) and yield strength (YS) of the two alloys under the second peak are significantly higher than these on the first peak. After solution-aging treatment, the maximum values of hardness, tensile strength and yield strength were 203 HB, 700.2 MPa and 601.9 MPa, respectively. But the elongation of the two alloys decreases with increasing aging time and the alloy without Sc have the larger breaking elongation. SEM observation of tensile fracture surfaces show that numerous dimples can be obviously observed over the entire surfaces, which have different size and shapes. Furthermore, there are cleavage and quasi-cleavage characteristics on the fracture surface. Thus, the fracture characteristic of Al-Zn-Mg-Cu-Zr(-Sc) alloys is a mixed ductile-brittle fracture. Comparing with the Al-Zn-Mg-Cu-Zr alloy, the alloy with Sc have the higher brittleness due to the higher strength with the addition of Sc. The observation results of TEM show that large amounts of η′ precipitates are homogeneously distributed in grain interior and some rod like precipitates are distributed discontinuously along grain boundaries in Al-Zn-Mg-Cu-Zr alloy. Besides, there also existed lots of fine Al_3(Sc, Zr) particles in Al-Zn-Mg-Cu-Zr-Sc alloy. The abundant nanometer-sized Al_3(Sc, Zr) particles effectively pined dislocations and subgrain boundaries, exhibiting excellent antirecrystallization behavior and precipitates strengthening effect. The grain refinement strengthening and precipitation strengthening play a dominant role in the additional strength of the Al-Zn-Mg-Cu-Zr-Sc alloy.

Keywords: Al-Zn-Mg-Cu alloy, aging treatment, mechanical property, fracture feature, microstructure

Influence of natural aging on precipitation hardening behavior of Al-Mg-Si-Cu alloys and their composites

Shize Zhu, Dong Wang, Bolv Xiao, Quanzhao Wang, Zongyi Ma
(Institute of Metal Research, Chinese Academy of Sciences)
blxiao@imr.ac.cn

Abstract: For engineering materials, excellent cold workability and high strength are expected. Based on Al-Mg-Si-Cu alloys and their composites, the aim can be reached by cold deformation during natural aging, and service after artificial aging. But this strategy means that materials will experience natural aging before artificial aging. Therefore, there is a considerable industrial and academic interest in understanding how natural aging affects the precipitation hardening behavior of Al-Mg-Si-Cu alloys and their composites. In this study, the nominal content of alloys is Al-1.2Mg-0.6Si-1.0Cu (in weight fraction), and composites are reinforced with 17% (in volume fraction) SiC particles. Both alloys and composites were fabricated by power metallurgy process and hot extruded. The extruded bars were solution treated at 540 ℃ and water quenched. Part of the quenched samples was artificially aged immediately at 170 ℃ for various time (named as AA-alloy, AA-composite, respectively), the rest of samples were naturally aged for 2 weeks, then artificially aged using the same parameters (named as NA-alloy, NA-composite, respectively). The tensile test was used to compare the influence of natural aging on mechanical properties of alloys and composites. It is showed that compared with AA-composite, not only is the peak ultimate tensile strength (named peak UTS) of NA-composite reduced, but the time to arrive at peak UTS is prolonged as well. This phenomenon is called the "negative influence" of natural aging. However, when composites are over-aged, the difference of UTS (named over UTS) between NA-composite and AA-composite is narrowed. After artificial aging for 24 hours, the over UTS of NA-composite is nearly the same as the AA-composite's. The "negative influence" of natural aging can also be found in alloys. But compared with the phenomenon in composites, the drop of peak UTS is more significant. What is more, in contrast to composites, given longer artificial aging time, the difference of over UTS between NA-alloy and AA-alloy become more obvious than the difference of peak UTS. Differential scanning calorimetry (DSC) analysis shows that different performance of "negative influence" of natural aging on composites and alloys results from different precipitation evolution. Thermoelectric power (TEP) and transmission electron microscopy (TEM) was used to analyze the mechanisms for the above results in details.

Keywords: metal matrix composite, Al-Mg-Si-Cu alloy, natural aging, artificial aging, precipitation hardening

Aging strengthening mechanism and thermal deformation of CuMg alloy

Bingjie Wang[1], Yi Zhang[1], Baohong Tian[1], Kexing Song[1], Huili Sun[1], Yong Liu[2]
(1. School of Materials Science and Engineering, Henan University of Science and Technology; 2. SUN)
lywbj126@126.com

Abstract: To investigate the aging strengthening mechanism and thermal deformation behavior of Cu-Mg alloy , aging treatment and thermal deformation were carried out. The Cu-Mg alloy were cast in a vacuum induction furnace in the graphite crucible at 1200 ℃, and then poured into the low carbon steel mold with Φ85 mm x 120 mm dimensions. Then the ascast ingots were squeezed into bars with 35 mm diameter by the XJ-500 metal profile extrusion machine at 900 ℃ for 1 h. Aging behavior of Cu-Mg alloy was studied after the solid solution at 850 ℃ for 2 h and cold deformation was carried out on a C33150-type laminating machine in different degrees of 20%, 40% and 80%, respectively. And then aged at 400, 420, 440, 460 and 480 ℃. Electrical resistance of the specimens was measured using a ZY9987 digital micro ohm meter. The phase transformation kinetics, electrical equations and TTT curve for the Cu-Mg alloy were established.

Morever, thermal deformation behavior of Cu-Mg alloy were investigated by isothermal axial compression tests using the Gleeble-1500D digital controlled dynamic simulation machine in the temperature range of 500-850 ℃ with the strain rates from 0.001 to 10 s^{-1}. The true stress-true strain curves under various deformation conditions were obtained from the tests. Based on the dynamic material model, hot processing maps of Cu-Mg alloy were established. The hot workability of the alloy was analyzed combining with the microstructural evolution of the Cu-Mg alloy. The specimens were polished and then etched with corrosive liquid of $FeCl_3$ (5 g) + HCL (10 mL) + distilled water (100 mL) and analyzed by optical microscope. The compressed specimens with ϕ8 mm×12 mm dimensions were compressed by the Gleeble-1500D thermo-mechanical simulator. Prior to compression, the samples were heated to the experimental temperature at 10 ℃/s rate and then kept at test temperature for about 3 min.

The results show that Cu-Mg alloy is temperature and strain rate sensitive alloy. Dynamic recovery and recrystallization are the main softening mechanism during the thermal deformation. At 460 ℃ aging, the earliest and the precipitation time is the shortest by TTT curve. After aging treatment, the hardness and electrical conductivity is improved. Furthermore, the flow stress increases with the decrease of temperature or the increase of strain rate. High temperature and low strain rate are beneficial to promote the dynamic recrystallization process. The temperatures from 630 to 815 ℃ and strain rates ranging from 0.001 to 0.1 s^{-1} are the proposed optimal processing parameters of Cu-Mg alloy.

Keywords: Cu-Mg alloy, aging treatment, thermal deformation, flow stress, dynamic recrystallization, hot processing maps

Effect of heat treatment on microstructure and properties of Ti6Al-4V-0.5Si alloy

Leiming Guo, Wenyan Wang
(Henan University of Science and Technology)
wangwy1963@163.com

Abstract: The effect of heat treatment on the microstructure and properties of Ti-6Al-4V-0.5Si alloy produced by powder metallurgy was investigated. In this experiment, the raw materials are composed of titanium powder, aluminum powder, vanadium powder and silicon powder with a purity of 99.9% and a particle size of 50 μm, which were mixed for 24 hours by mixed element method in the Y mixer. During the cold isostatic pressing process, the mixed powder was compressed into cylindrical embryos under a pressure of 150 MPa and a dwell time of 3 min. The cylindrical Ti-6Al-4V-0.5Si alloy rod with a diameter of 40 mm and a high of 110 mm was obtained by the vacuum sintering process with vacuum degree of 1×10^{-5} Pa. The sintering temperature curve is shown in Figure 1. The Ti-6Al-4V-0.Si alloy was treated by solid solution ageing in the SX-10-13 muffle furnace. Heat treatment process is shown in table 1. The alloy after heat treatment was grinded, polished and corroded. The corrosion agent is Kroll solution and corroded time is about 15-20 s. The metallographic microstructures were analyzed by a XJG-05 metallographic microscope. The micro-hardness was tested by a MH-3 micro-hardness tester with load of 200 g. The mechanical properties were tested by a SHIMADZU AG-I 250 KN precision universal testing machine. The fracture morphologies were analyzed by a JSM-5610LV model scanning electron microscope and the phases were analyzed by a Brux D-8 X ray diffractometer and a JEM-2100 model transmission electron microscopy. The results show that with the increase of the solid solution temperature, the tensile strength of Ti-6Al-4V-0.5Si alloy increased initially, followed by a decrease. There was an increase of tensile strength about 15% under the solid solution temperature of 950 ℃. In the as-cast state, the tensile strength of the alloy is 710 MPa, and the tensile strength is 820 Mpa after solid solution aging. The tensile strength of Ti-6Al-4V-0.5Si alloy decreased as the aging temperature increases, but the plasticity of the alloy increased greatly. Martensitic structure was produced in the alloy matrix after solid solution. After aging, the martensitic structure is decomposed and the dispersed α+β phases were obtained. By optical microscope analysis, it was found that the grain boundaries of the structure were straighter and clear, indicating that the process of dynamic recrystallization and grain growth occurred during heat treatment. Through SEM analysis of the fracture, a small amount of dimples was found in the section and the fracture mechanism of the material was quasi-cleavage fracture. By XRD and TEM analysis of the phase, the main precipitates are α phase and β phase, and the dispersion phase Ti_5Si_3 in the structure. Ti_5Si_3 can increase the nucleation rate and inhibit the grain growth. Comprehensive analysis shows that the comprehensive performance of Ti-6Al-4V-0.5Si alloy is optimal at the solid solution temperature of 950 ℃×30 min (WQ)+480 ℃×4 h (AQ).

Keywords: Ti-6Al-4V-0.5Si alloy, solid solution aging, tensile strength, elongation

Characterization and corrosion behavior of a laser surface quenched nickel-aluminum bronze

Zhenbo Qin[1], Zhong Wu[2], Lei Liu[1], Wenbin Hu[2]
(1. State Key Laboratory of Metal Matrix Composites, Shanghai Jiao Tong University;
2. School of Material Science and Engineering, Tianjin University)
wuzhong2319@163.com

Abstract: Nickel-aluminum bronze (NAB) alloy is a copper–aluminum alloy with addition of aluminum, nickel, iron and manganese elements. It is widely used as propeller in marine environments, due to the excellent combination of mechanical properties and corrosion resistance. The present manufacture of propeller is mainly sand casting, leading to the existence of grain coarsening and composition segregation defect. To homogenize the organization, improve tenacity and enhance anti-fatigue performance, the propeller is general annealed integrally before serving. However, annealing reduces the strength of the material and weakens the cavitation corrosion resistance. In addition, metallurgical complex microstructure are prone to suffer selective phase corrosion, which forms a serious local corrosion and lays down safety hazards for the service of the workpiece.

It is generally accepted that the corrosion is mainly occurred at the surface, so the corrosion properties are determined by the surface structure of the alloys. On the premise of not changing the overall mechanical properties of the workpiece, surface treatment can be applied to modify the surface microstructure. In this way, the fatigue property of propeller can be guaranteed, and the corrosion resistance of static corrosion and cavitation can be improved simultaneously. The optimum corrosion resistance can be obtained by controlling the composition, as the corrosion resistance of NAB alloy depends strongly on their microstructure.

Previous researches have focused on the effect of microstructure evolution in improving the corrosion fatigue performance of the components, and neglected the influence of the corrosion properties by the change of the microstructure. In this study, laser surface quenching technology was used to prepare modified surface layer on as-cast NAB alloy. By adjusting the process parameters, a modified layer containing surface fine grain zone and heat affected zone was obtained on the alloy surface. The modified microstructure in the fine grain zone was relatively uniform and small, which showed extremely tiny κ phase precipitated in acicular β phase. The depth of the fine crystalline region was about 220 μm, and the hardness was improved to 430-440 HV.

Electrochemical measurements and static immersion corrosion test were used to investigate the corrosion behavior after laser surface quenching. Due to the refined and homogenized microstructure, selective phase corrosion was eliminated, and the corrosion rate was reduced by about 42.5%. Meanwhile, nickel and aluminum were supersaturated and distributed evenly in the quenched microstructure, which in turn promoted the rapid formation of a protective corrosion production film, and reduced the corrosion rate. In addition, attributed to the improved hardness and homogeneous microstructure of the fine crystalline region, the synergy of mechanical erosion and electrochemical corrosion was small, and cavitation corrosion resistance of nickel-aluminum bronze alloy increased by a factor of 8.8.

Keywords: nickel-aluminum bronze alloy, selective phase corrosion, laser surface quenching, cavitation corrosion

Preparation of ZrB_2 particle reinforced Cu matrix composites from both ex-situ and in-situ routes

Zhiguo Zhang, Chenchen Wang, Wei Li
(Institute of Advanced Wear and Corrosion Resistant and Functional Materials, Jinan University)
zhigzhang@jnu.edu.cn

Abstract: Metal matrix composites (MMCs) have received increasable interest over the last several decades and have emerged as an important class of engineering materials. Zirconium boride reinforced copper composites (ZrB_2/Cu) demonstrate great potential structural and functional applications in aerospace, automobile, and electric power cable industries because of their high specific strength, specific modulus, and good wettability between ZrB_2 and molten copper. However, the understanding of the different process parameters on the composite microstructure, electrical properties as well as the mechanical properties is still limited.

In this study, the ZrB_2/Cu composites were prepared via both the ex-situ and in-situ methods. The ex-situ method combines a milling and sintering process. The effects of various powder metallurgy parameters such as the ZrB_2 reinforcement contents, the sintering temperature on the microstructure and mechanical and electrical properties were studied in details. On the other hand, the in-situ methods are through the reaction between elemental Zr and B in liquid copper. XRD, Raman, SEM and TEM are used to characterize the microstructure of the prepared composites. The mechanical and electrical characteristics were also measured.

The research results in the ex-situ method show that the relative density and electrical conductivity of the composites decrease with increasing ZrB_2 content. However, the microhardness reaches a maximum value of 100.8 HV0.2 as ZrB_2 content increases to 7wt% and then decreases when ZrB_2 content further increases. The hexagonal ZrB_2 crystals in size of several micrometers are well embedded in Cu matrix. Grain refinement strengthening, Orowan strengthening and coefficients of thermal expansion mismatch strengthening contribute to the increment of microhardness and reduce the electrical conductivity. It is also found that the relative density and electrical conductivity of the composites are improved with the increase of sintering temperature. The microhardness of the composites increases firstly and then decrease. A maximum microhardness of 92 HV0.2 is achieved at 840 ℃. The grain growth of Cu matrix with the increase of sintering temperature is confirmed by XRD and SEM.

The results from the in-situ method indicate that ZrB_2 particles can form through the reaction of Zr and B in molten Cu (1300 ℃). The obtained composites consist of hexagonal shaped ZrB_2 and Cu(Zr) solid solution matrix. The obtained ZrB_2/Cu composites exhibit improved microhardness. However, the electrical conductivity decreases with increasing weight fractions of ZrB_2. In both studies, the interfacial zone between ZrB_2 particle and Cu matrix consists of both sharp interfaces and amorphous transition layer.

Keywords: mechanical property, electrical conductivity, copper matrix composites, ZrB_2, interface structure

Surface modification of the NAB alloy to improve the corrosion resistance and cavitation erosion resistance via thermal diffusion process

Zhong Wu[1], Qin Luo[2], Wenbin Hu[1]
(1. School of Material Science and Engineering, Tianjin University;
2. State Key Laboratory of Metal Matrix Composites, Shanghai Jiao Tong University)
wuzhong2319@163.com

Abstract: The surface modification of nickel-aluminum bronze alloy (NAB) was developed by thermal diffusion of Ni coating and the alloy matrix, which was designed as the outer gradient layer of Ni-Cu solid solution and the inner layer of Ni-Al-Cu intermetallic by means of intrinsic properties of the triple diffusion system of Cu, Ni and Al. Cu atoms diffused faster than Al atoms within Ni matrix, which resulted in the continuous accumulation of Al atoms in the inner layer to generate the Ni-Al-Cu intermetallic, and the Ni-Cu solid solution acted as the outer layer. Optimization of the thickness of Ni coating, the temperature and the heat treatment time, the completely gradient Ni-Cu layer and the Ni-Al-Cu layer were obtained. The enhanced corrosion resistance of Ni-Cu layer could be found in the salt spray test, which exhibited local corrosion with uniform corrosion compared with severe selective phase corrosion of the NAB alloy and pitting corrosion of Ni-Al-Cu layer. According to the electrochemical tests, the improvement corrosion resistance of the gradient Ni-Cu layer was due to the formation of protective film, which mainly consisted of $Ni(OH)_2$ and Cu_2O. The vertical growth of the pits was depressed and the uniform corrosion was promoted. When pits are formed on the surface, galvanic corrosion occurred simultaneously. The driving force for the galvanic corrosion comes from the potential drop between the outer passive layer and the bare Ni-Cu in the pits. With the gradient distribution of Ni-Cu layer, the corrosion potential presents gradient variation. Thus, the interfacial potential drop in the pits was decreased and the driving force for galvanic corrosion was relieved. According to the SVET results, the anodic dissolution of the gradient Ni-Cu layer was more difficult compared to that of the NAB alloy. Thus, the ions concentration within the pit electrolyte of the gradient Ni-Cu layer was less than that of the NAB alloy. It means that the ohmic potential drop within the pit electrolyte of the gradient Ni-Cu layer was higher, and the corrosion rate was lower. The microstructure of the Ni-Al-Cu layer was homogeneous with a refined grain size of about 3 μm. Nano-indentation hardness of the Ni-Al-Cu layer was about 5.5 GPa, almost two times as large as the NAB substrate, which was due to the precipitation of hardened Ni3Al phase. With cavitation erosion test for 12 h, the cumulative mass loss of the NAB alloy was about 6.4 times and 5.5 times as large as that of the Ni-AlCu layer in distilled water and 3.5wt% sodium chloride (NaCl), respectively. Electrochemical measurements under quiescence and cavitation erosion conditions were conducted to investigate the synergistic effects of cavitation erosion and corrosion. The percentage of the erosion component of the NAB alloy and the Ni-Al-Cu layer was over 80%, which indicated that the main damage was caused by the erosion factor. The improving cavitation erosion-corrosion resistance of the Ni-Al-Cu layer was mainly due to the homogeneous and refined microstructure with increasing hardness. Besides, the synergism had measurable effect on the cavitation erosion-corrosion process for the NAB alloy and the Ni-Al-Cu layer. And the synergism of WCIE+WEIC for the Ni-Al-Cu layer was bigger than that of the NAB alloy.

Keywords: nickel-aluminum bronze allo, gradient Ni-Cu layer, Ni-Al-Cu layer, electrochemical calculation, SVET, passive films, cavitation erosion

Evolution of electrical conductivity, hardness and strength during age hardening of AA7010

Yuyuan Zhao
(University of Liverpool)
zhaoyy@liv.ac.uk

Abstract: AA 7010 is one of the main structural Al alloys used in structural components in the aircraft industry, e.g. the wings of Airbus aircraft. Many of the structural components are machined and overheating can be induced during machining due to blunt cutters, lack of lubrication or excessive removal of material. Overheating is manifested by decreases in electrical conductivity and hardness, so combining these two properties provides an effective, non-destructive monitoring and inspection method. This presentation reviews the correlations between electrical conductivity and hardness and the relationships between strength and hardness for AA 7010. Strong correlations exist between hardness and electrical conductivity over natural, artificial and over ageing regimes with a wide range of ageing time. Electrical conductivity can be used to detect over ageing, but it alone cannot predict hardness. Combining electrical conductivity and hardness values can be used to predict thermal history. Two independent sets of data demonstrated that there are linear relationships between hardness, yield stress and tensile strength. The hardness-yield stress relationship can be justified by the constraint factors calculated using contact mechanics models and the work hardening taking place during hardness testing.
Keywords: electrical conductivity, hardness and strength, AA7010 alloy

Effect of nitrogen content on microtructure and mechanical properties of multi-element (AlCrTiZrV)N films by reactive magnetron sputtering

Chunke Huang, Wei Li, Ping Liu, Fengcang Ma, Ke Zhang, Xiaohong Chen, Xinkuan Liu, Daihua He
(University of Shanghai for Science and Technology)
liwei176@usst.edu.cn

Abstract: The multi-component (AlCrTiZrV)N films were deposited from a single high entropy alloy target by reactive magnetron sputtering under a mixed atmosphere of Ar and N_2. The composition, microstructure and mechanical properties of the films prepared at different N2-to-Ar flow ratios were investigated. The AlCrMoTaTiZr metallic film deposited at the N_2 flow of 0 shows an amorphous structure, while the (AlCrTiZrV)N films synthetized at the N_2-to-Ar flow ratios of 1:2, 3:4, 1:1, 5:4 and 3:2 present a simple face-centered cubic solid solution structure. With the increase of N_2 flow, the hardness and elastic modulus of the (AlCrTiZrV)N film firstly increase and then decrease. When N_2-to-Ar flow ratio is 3:4, the hardness and modulus reach a maximum value of 34.9 GPa and 356 GPa, respectively. The multi-element (AlCrTiZrV)N nitride films have potential in hard coating applications.
Keywords: multi-element nitride film, microstructure, mechanical property, strengthening mechanism, magnetron sputtering

Effect of cryogenic treatment technique on microstructure and mechanical property of spray 7055 alloy

Guoxing Pang
(School of Material Engineering, North China Insititute of Aerospace Engineering)
panglfht@163.com

Abstract: The effects of cryogenic treatment technique on the microstructure and properties of spray 7055 alloy were investigated using mechanical properties tests, electric conductivity tests and microstructure observation. The results show that the alloy properties can be stable with cryogenic recycle treatment, but the effect of property improvement is not obvious with times increasing of cryogenic recycle treatment. The spray 7055 alloy is with the better properties after treatment of solution treatment, one time cryogenic treatment, and three times aging treatment, and the properties index obtained as below: tensile strength 685.2 MPa, elongation 15.5%, hardness 191 HB, electric conductivity 37.2%IACS.

Keywords: cryogenic treatment, microstructure, property, spray 7055 alloy

Study on the effect of cryogenic treatment on the microstructure and hardness of Ti-6Al-4V with the application of synchrotron X-ray diffraction

Yichen Meng, Matteo Villa, Thomas Christiansen, Kristian Dahl, Marcel Somers
(DTU)
somers@mek.dtu.dk

Abstract: Ti-6Al-4V was (intercritically) annealed in the temperature range 1000-1250 K with intervals of 50 K, followed by cooling to room temperature at an average rate of approx 1 K, s1. The heat treatment procedure was intended to systematically vary the microstructure and alter the thermal stability of the β phase though the partitioning of the alloying elements between α and β phases during the annealing step. The annealing treatment was followed by cryogenic treatment, which consisted of immersion in boiling nitrogen for various durations ranging from 5 minutes to 24 hours, followed by re-heating in air. The heat treated material was characterized ex situ applying optical microscopy (OM), synchrotron X-ray diffraction (XRD) and hardness measurements. A set of samples was not subjected to cryogenic treatment and was taken as reference. OM revealed that the material microstructure after heat treatment consisted of various fraction of primary α grains and regions of lamellar α/β structure. XRD showed that the fraction of retained β was the largest, approx. 4%, for the material treated at the highest applied annealing temperature, i.e. 1250 K, and decreased to 2% with a reduction of the annealing temperature. Hardness values in the range 300-330 HV were obtained, showing no direct effect of the annealing temperature. The applied techniques did not reveal any measurable effect of cryogenic treatment, neither on the microstructure, nor on the hardness. This fact is inconsistent with literature data and is interpreted in terms of a pronounced partitioning of the alloying elements during the formation of lamellar α/β structure on (moderately) slow cooling from the annealing temperature, which induces enhanced stability of the retained β phase against its conversion into martensite during cryogenic treatment.

Keywords: titanium alloy, Ti-6Al-4V, heat treatment, phase transformation, cryogenic treatment, synchrotron X-ray diffraction

In vitro biocorrosion behavior of as-cast biodegradable Mg-Zn-ZrGd alloy

Ya Liu, Jiuba Wen, Junguang He
(Henan University of Science and Technology)
liuya_021@163.com, wenjiuba12@163.com

Abstract: The in vitro biocorrosion behavior of as-cast biodegradable Mg-0.5Zn-0.4Zr-5Gd alloy was investigated in simulated body fluid (SBF). The corrosion behavior of the alloys with different immersion times was studied by means of weight loss test, hydrogen evolution, the corrosion microstructure observation and electrochemical test. The as-cast Mg-0.5Zn0.4Zr-5Gd alloy compose of dendrite α-Mg matrix together with lots of discontinuous netted eutectic compounds. In the initial stage about 8 h immersion, the corrosion rate is higher and more hydrogen is produced due to the reaction of magnesium and Cl^- ion. Meanwhile, white rounded volcano-like shape was observed on a fraction of the corrosion layer. After 4 days immersion, the rate of corrosion has become more stable. After a period of 5 days of immersion times, corrosion products become more and form a thicker corrosion layer. The corrosion films which is mainly composed of $Mg(OH)_2$, $Ca_{10}(PO_4)_6(OH)_2$ and $(Ca, Mg)_3(PO_4)_2$ provide a protection for the alloy, so the corrosion rate gets lower with immersion time. As can be seen from the morphologies after removing corrosion products, the corrosive images are characterized by pitting corrosion and intergranular corrosion. In the early stage about 8 h of immersion, the surface of the sample is more smooth. However, from the immersion time of 5 days, there exists small pitting corrosion holes and large area of corrosion inhomogeneity. At the range of 1 days to 5 days, the diameter of high-frequency capacitive loop increases with immersion times related to the increasing protective inner MgO layer thickness in most of the area. After soaking in simulated body fluid for 5 days, the corrosion rate become stable and the corrosion resistance reaches the highest level from electrochemical test.

Keywords: magnesium alloy, simulated body fluid, in vitro, corrosion

Wear and corrosion behavior of graphene nanoplates reinforced copper matrix composites prepared by electrostatic self-assembly and powder metallurgy

Ke Zhang
(University of Shanghai for Science and Technology)
zhangke@usst.edu.cn

Abstract: Since the densities of copper and graphene nanoplates (GNPs) are different, it is one of the key challenges for the synthesis of graphene nanoplates/copper (GNPs/Cu) composites to disperse GNPs uniformly in the Cu matrix. In this work, GNPs/Cu composites were synthesized through electrostatic self-assembly and spark plasma sintering and the GNPs were uniformly dispersed in the copper matrix. The graphene protective films can be formed in the composites to protective the Cu matrix. The wear resistance of GNPs/Cu composites was investigated using the ball-on-disc apparatus, and the corrosion resistance of GNPs/Cu composites was estimated by the potentiodynamic polarization curves. Furthermore, the wear mechanism and corrosion mechanism have been analyzed using scanning electron microscopy with energy dispersive spectroscopy. It was found that the wear resistance and corrosion resistance of the composites can be significantly improved through the addition of GNPs.

Keywords: copper matrix composites, graphene nanoplates

Quantitative evaluation of porosity in Al-Si-Cu die casting cylinder block

Xuan Wang[1], Chen Liu[1], Wentao Zhou[2], Zhongyang Liang[1], Zhenbo Zhao[3], Hua Gao[3]
(1. College of Mechanical Engineering, Yangzhou University, Jiangsu;
2. College of Mechanical Engineering, Yangzhou University, Jiangsu;
3. Sensus Precision Die Casting (Yangzhou) Co., Ltd., Jiangsu)
yzu_WangXuan@163.com, liuch@yzu.edu.cn, 1209705023@qq.com, 2579223889@qq.com

Abstract: Aluminum alloys have been steadily spotlighted as a potential material for the achievement of weight reduction in the automobile and aerospace industry because of excellent castability and high specific strength. In the die-casting process, the formation of pores in components is hard to avoid. Porosity has a harmful effect on the strength and pressure tightness of die castings and is becoming a fairly common complaint of casting users and heightens customer concerns about part reliability and quality. To this respect, the evaluation of relationship between strength and porosity is an important aspect to improve the quality of complex castings for further applications. In the present study, fractured surface analysis is proposed to characterize porosity in terms of the morphology, size and distribution in a commercial Al-Si-Cu cylinder block. A quantitative estimation of the influence of porosity on tensile strength is investigated, which can be expressed by a formula of (f is the area fraction of the porosity, σ_0 is the maximum tensile strength in the condition of no porosities and α is the imperfection sensitivity of tensile strength). It indicates that both ultimate strength and elongation show a strong dependence upon the quantitative variation in porosity, with a linear and inverse parabolic relationship, respectively. It has been further confirmed that the surface rather than volume porosity in the equation can more effectively predict the overall degradation of tensile properties in the aluminum alloy die castings.

Keywords: die casting, Al-Si-Cu alloy, quantitative evolution, porosity, fracture surface

Effect of thermo-mechanical treatments on the microstructure and mechanical properties of in situ TiB reinforced Ti matrix composite

Fengcang Ma, Ping Liu, Wei Li, Xinkuan Liu, Xiaohong Chen, Ke Zhang
(University of Shanghai for Science and Technology)
mafengcang@163.com

Abstract: TiB reinforced Ti titanium matrix composite (TMC) was fabricated using in situ technologies. Effects of thermo-mechanical processing on microstructure and realignment effect of TiB whiskers in the composite were investigated. Mechanical properties variation by this treatment was measured, and strengthening effects of microstructure refinement and TiB whiskers were evaluated by models. It was found that the microstructure of the composite is refined significantly by the thermo-mechanical processing due to the recrystallization of prior beta grain. With the increase in deformation amplitude, the value of probability density function of small orientation angles of TiB whiskers increases sharply. Strength of the composite is increased significantly by the thermo-mechanical processing, which result from the increase in the strengthening effect of TiB whisker and the microstructure refinement. The value of the thickness of alpha plates without precipitated sillicides has minor effect on the strength of the composite but it becomes a non-ignorable strengthening factor after precipitation of sillicides due to the dislocation hindering of sillicides.

Keywords: fibers reinforced TMC, microstructure refinement, mechanical property, strengthening effect, thermo-mechanical processing

The influence of ω phase on super refined α precipitations in Ti55531 alloy

Hui Shao, Minjian Zhao
(Xi'an University of Technology)
904629056@qq.com

Abstract: Ti-55531 (Ti-5Mo-5Cr-5V-3Al-1Zr) is a new near-beta titanium alloy, owning to the high tensile strength (≥1200 MPa), good fracture toughness (55 MPa·$m^{1/2}$) and hardenability (≥250 mm). It is noteworthy that Tβ temperature of this alloy is lower compared to similar alloys (Ti-5553, Timetal 555,VT 22), which is attractive for the forging industry and employed in the airframes of A380 airplanes. The mechanical property of titanium alloy strongly depends on the volume fraction, morphology, size and distribution of α phase within the β matrix. In recent years, it is reported that the isothermal ω phase can enhancing the homogeneous nucleation of α precipitates with a fine-scaled size. However, little works has been focused on ω assisted precipitation behavior of α phase.

In this study the precipitation behavior of ω assisted α phase and its effect on hardness were investigated by two-step aging heat treatments. Surface hardness was measured by HR-150A Rockwell Hardness Tester with a test load of 150 kg and dwell time of 15 s. The microstructure of sample was observed by the OLYMPUS optical microscope (OM), JSM-6301F field emission scanning electron microscope (SEM) and transmission electron microscope (TEM). For OM and SEM observations, samples were mechanically polished and etched using the solution of hydrofluoric acid (10 mL), hydrogen nitrate (20 mL) and deionized water (50 mL). TEM samples were prepared by hand grinding and two Jet thinning.

In conclusion, a large number of isothermal ω phases are precipitated by low-temperature aging processes (300-400 ℃). The hardness values of alloys increase with increasing the size of ω phase. After the subsequent high-temperature aging processes (580 ℃), the ω-assisted α precipitations have different morphologies with α laths and α colonies. The hardness values of alloys increased by sixty precent, comparing with the low-temperature aging processes. The uniform precipitation of super refined α phases with few α colonies is obtained by aging at 300 ℃ for 12 h and following at 580 ℃ for 5 h.

Keywords: Ti-55531 titanium alloy, isothermal ω phase, age-hardening

Preparation and gas sensitive properties of SnO_2 nanowires

Jianhui Li
(Hebei University of Science and Technology)
85739435@qq.com

Abstract: SnO_2 nanowires were synthesized by thermal evaporation of Sn at a low vacuum. The as-grown nanowires were characterized by X-ray diffraction, scanning electron microscopy, transmission electron microscopy. The results showed that the nanowires match the rutile structure, grow along the [101] direction, are about 70 nm in diameter. The gas sensing tests of SnO_2 nanowires sensor have been conducted. The results showed that, the optimal operating temperature of the SnO_2 nanowires sensor is 300 ℃, and the sensor shows excellent sensitivity and fast response/recovery characteristics.

Keywords: SnO_2, nanowires, thermal evaporation, gas sensitive properties

Forming limits of sheet metals of different tempers in incremental forming

Ghulam Hussain[1], Xiaofan Xi[2], B. B. L. Isidore[3]
(1. GIK Institute; 2. Shanghai University of Engineering Science;
3. Lehrstuhl Konstruktion und Fertigung)
gh_ghumman@hotmail.com

Abstract: Incremental forming (SPIF) is an innovative metal forming process with high economic payoff. The forming limit (or formability) in this process can be maximized by employing a tool having radius of 2.2 times of sheet thickness (i.e., $R_c \approx 2.2T_0$ where R_c is the critical tool-radius and T_0 is the sheet thickness). However, this condition is valid for sheet metals of 1 mm thickness and step size of 0.2 mm. In the present study, a more generic condition is developed by varying the sheet thickness and step size over a range. A number of materials of different tempers are formed to fracture and formability trends as function of normalized radius (i.e., $R/T_0=R$) are deduced. It is found that the critical tool-radius increases from 2.2 to 3.3 as the thickness of sheet is increased from 1 mm to 3 mm. However, its value remains insensitive to variation in step size (i.e., from 0.3 mm to 0.7 mm). This is also observed that the selection of tool with $R<R_c$ narrows down the formability window on higher as well as lower side. The higher limit, as revealed by experiments and FEA, narrows due to excessive shearing because of in-plane biaxial compression, and the lower limit contracts due to pillowing of sheet metal. The more generic toolradius condition proposed herein study would be helpful in maximizing the formability of wide range of materials in SPIF without making trial and error. Moreover, this study offers a new level of understanding on the formability-tool size relationship in SPIF.

Keywords: incremental forming, temper, finite element analysis, formability, tool size

Effects of compositions on localized corrosion in Al-Zn-Mg-X Al alloys

Yingying Jia, Li Liu, Jiantang Jiang, Liang Zhen
(Harbin Institute of Technology)
jjtcy@hit.edu.cn

Abstract: Effects of compositions on localized corrosion in Al-Zn-Mg-X alloys were studied in the current research. The microstructure, microchemistry, pitting and intergranular corrosion (IGC) were characterized using SEM, EBSD, TEM and EDS. The localized corrosion were studied by polarization tests, exfoliation corrosion susceptibility tests (EXCO) and slow strain rate tensile tests (SSRT).The study shows that the addition of Sc to Al-Zn-Mg-Cu alloy can inhibit recrystallization and reduce the grain boundary misorientation of the recrystallized microstructure. Reduced PFZ width as well as suppressed solute segregation in grain boundaries precipitates was observed as 0.2wt% Sc added. Polarization curves suggests that the breakdown potential and current density descends in order of 7050>Al-ZnMg-Cu-Sc-Zr (MCuSc)>Al-Zn- Mg-Sc-Zr (MSc). The addition of Sc decreases the breakdown potential of 7050 alloy and the removal of Cu is the main cause for the decrease in corrosion potential. EXCO tests show that IGC susceptibility of these alloy decrease at the sequence: 7050>MCuSc>MSc. Only slight pitting was observed in MSc after 15 hours EXCO test, indicating an excellent IGC resistance. SSRT tests showed that SSC sensitivity decrease at the sequence: 7050>MCuSc>MSc. The addition of Sc and the removal of Cu is believed enhance the SCC resistance. The study shows that the addition of Sc, the removal of Cu combined with proper aging process can enhance the corrosion resistance of 7xxx series alloys.

Keywords: Al-Zn-Mg-*x* alloy, composition, microstructure, microchemistry, localized corrosion

Effect of friction stir processing on microstructure and mechanical properties of Al-Mg-Si alloy

Feifei Liu, Yongqiang Qin, Yeming Hu, Shiang Zhou, Hongmei Zheng, Yucheng Wu
(School of Materials Science and Engineering, Hefei University of Technology)
albon@hfut.edu.cn, zhoushiang88@163.com, ycwu@hfut.edu.cn

Abstract: In this present work, friction-stir processing (FSP) were carried out on Al-Mg-Si alloy under the solid-solution and aging states. Effect of FSP and heat treatment processes on microstructure and mechanical properties of the alloy were systematic investigated by means of OM, EBSD, TEM, micro-hardness and room-temperature tensile testing. After FSP, the solution-treated and aging-treated alloys exhibited a typical structural character of fine, equiaxed and fully recrystallized grains with a size of about 10 μm and imposed a significant softened effect. The same values of mechanical properties of the two alloys indicated that pre-treatment had little effect on Al-Mg-Si alloy subjected to FSP. The micro-hardness of the as-processed alloys increased gradually with the increasing aging time and the highest value was obtained when aging-treated for 6 h at 180 ℃. An outstanding comprehensive property of ultimate tensile strength (411 MPa), yield strength (345 MPa) and elongation (17.2%) was obtained.

Keywords: Al-Mg-Si alloy, friction-stir processing, mechanical properties, aging-treated

The corrosion behavior of Mg-2Nd-0.5Zn-0.4Zr-1Y alloy

Dazhao Xu, Junguang He, Jiuba Wen, Lige Zheng
(Henan University of Science and Technology)
he.ellen@163.com

Abstract: The degradable behavior of Mg-2Nd-0.5Zn-0.4Zr-1Y alloy in simulated body fluid (SBF) was investigated in different immersion time by means of immersion tests, EDS and electrochemical measurements. The results showed that white aggregates appeared on the surface during a short immersion time. As the immersion time increases, the alloy corrodes seriously and forms more aggregates. The surface of the alloy begins to become nonsmooth. EDS results show that the corrosion production contain phosphate, oxides and $Mg(OH)_2$. The impedance increases during a short immersion time and reaches a maximum value in 1d and then the impedance decreases. Inductive loops occur when the alloy is soaked for 3 days and 10 days. The degradation behavior of alloy in SBF can be summarized as follows. The corrosion of alloy starts from the Zr-rich region. With the prolongation of immersion time, the Zr-rich region continues to corrode, generating $Mg(OH)_2$ and H_2. After a certain balance, $Mg(OH)_2$ dehydrates to form MgO. The hydrogen gas accumulates to a certain extent, thereby breaking down the corrosion layer and forming holes. Finally, the local corrosion morphology was formed.

Keywords: degradable behavior, immersion time, corrosion products, impedance

Strengthening effect of extruded Mg-8Sn-2Zn-2Al alloy: influence of micro and nano-size Mg_2Sn precipitates

Weili Cheng[1], Yang Bai[1], Lifei Wang[1], Hongxia Wang[1], Hui Wang[2]
(1. Taiyuan University of Technology; 2. Hebei University of Technology)
baiyanga0320@gmail.com

Abstract: In this study, Mg-8Sn-2Zn-2Al (TZA822) alloys with varying Mg_2Sn contents prior to extrusion were obtained by different pre-treatments (without and with T4), and the strengthening response related to micro and nano-size Mg_2Sn precipitates in the extruded TZA822 alloys was reported. The results showed that the morphology of nano-size Mg_2Sn precipitates exhibits a significant change in basal plane from rod-like to spherical, owing to the decrement in the fraction of micro-size particles before extrusion. Meanwhile, the spherical Mg_2Sn precipitates provided a much stronger strengthening effect than did the rod-like ones, which was ascribed to uniform dispersion and refinement of spherical precipitates to effectively hinder basal dislocation slip. As a consequence, the extruded TZA822 alloy with T4 showed a higher tensile yield strength (TYS) of 245 MPa, ultimate tensile strength (UTS) of 320 MPa and elongation (EL) of 26.5%, as well as a lower degree of yield asymmetry than their counterpart without T4. Detailed reasons for the strengthening effect were given and analyzed.
Keywords: Mg-Sn alloy, extrusion, strengthening

Study on power supply mode and loading parameters for magnesium alloy micro-arc oxidation

Jiantao Yao
(Xi'an Shiyou University)
jiantaoyao@xsyu.edu.cn

Abstract: Micro-arc oxidation (MAO) is a technology for non-ferrous metal surface treatment through growth ceramic layer on the original surface. In order to determine the influence of the power supply mode and the loading parameters on the film forming of magnesium alloy micro-arc oxidation processing, the different power supply modes of direct current, single-polarity pulse, double-polarity pulse and the pulse power supply with a discharge loop was used to micro-arc oxidation technology on the AZ91D magnesium alloy. The power load parameters are optimized. The average energy consumption is calculated. Results showed that the role of the negative voltage in the bipolar pulse power supply only is restrain the large arc tendency. Under the pulse power supply with a discharge loop, the current and energy consumption decreases with the increase of the discharge resistance at the same pulse parameters. The results indicate that the big arc phenomenon can be effectively avoid and the impact of load capacitance can be effectively eliminated by using the pulse power supply with a discharge loop. Moreover, the processing of the micro-arc oxidation is stable, the arc point is uniform, the surface of the film is smooth, the hole is uniform and dense, and the film efficiency is improved effectively. The power load parameters are optimized. The different voltage increments with the different stage of micro-arc oxidation.
Keywords: micro-arc oxidation, load characteristics, power mode

Preparation of Cu doped graphene reinforced Cu matrix composites and its microstructure and properties

Xiaohong Yang, Yu Chen, Juntao Zou, Peng Xiao, Shuhua Liang
(Shaanxi Key Laboratory of Electrical Materials and Infiltration Technology, School of Materials Science and Engineering, Xi'an University of Technology, Xi'an 710048, China)
yangxh@126.com

Abstract: Pure copper has good electrical conductivity, but its strength is not high. With the rapid development of rail transportation, electronics, machinery and other fields, the demand for high strength and high conductivity copper alloy is getting higher and higher. Copper alloy is easily softened at high temperature. So copper matrix composite has become a research hotspot. Graphene, a single layer sp^2-hybridized carbon atoms arranged in two-dimensional honeycomb crystals. Because of its unique structure, it has excellent mechanical properties, high conductivity and good thermal stability. Therefore, graphene as a reinforcement for preparing graphene/copper composites is expected to become a new generation of high strength and high conductivity materials.

In this paper, Cu doped graphene compound powders were synthesized by in situ chemical reduction method. Graphene oxide (GO) was used as the raw material to ultrasonic dispersion in deionized water to form a solution of graphene oxide. The copper salt solution (Cu $(NO_3)_2$ $3H_2O$) was added into the GO solution. After ultrasonic dispersion and magnetic stirring, the hydrazine hydrate was added to the water bath reduction. The Cu doped graphene were synthesized by centrifugal washing and vacuum freeze-drying. XPS analysis of the composite powder indicates that the main carbon bond in GO is C-O, and C-C is the main carbon bond after the in situ chemical reduction, and the graphene oxide is fully reduced during the reduction process. Through the observation of SEM morphology of the compound powder, it is found that Cu nanoparticles distribute evenly in the graphene sheets, which effectively blocks the agglomeration of graphene. The Cu doped graphene and copper powder were mixed in the anhydrous ethanol, the composite powder was dried in a magnetic stirring water bath after ultrasonic dispersion and magnetic stirring. The Cu doped graphene/copper matrix composites were prepared by cold pressing and sintering. It is found that graphene is embedded in copper matrix by SEM analysis. And then the density, electrical conductivity, and hardness of the composite were tested. The results show that when the addition Cu doped graphene is 0.5wt.%, the composite has better comprehensive properties, the electrical conductivity can reach 89%IACS, the Vickers hardness is 80.2 HV, which was 37% higher than that of pure copper prepared by the same process parameters.

Fig.1 shows the SEM images of Cu-doped graphene compound powders. It can be seen from the picture that the white spherical particles are copper nanoparticles by in situ generated, and the thin sheets with wrinkled structure and transparent shape are graphene. And graphene shows obvious wrinkle structure.

Keywords: graphene, Cu doped graphene, Cu matrix composites, Vickers hardness

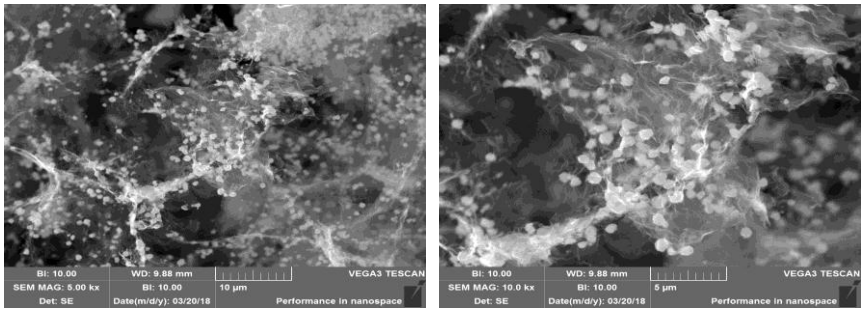

Fig.1 SEM images of Cu-doped graphene compound powders

Microstructural evolution and mechanical properties of Ti-6Mo-5V-3Al-2Fe alloy aged at various temperatures

Rui Wang, Xuemeng Wang, Haoyu Zhang, Lijia Chen
(Shenyang University of Technology)
478155422@qq.com

Abstract: Due to their high specific strength, good match between strength and plasticity, β-titanium alloy is one of the most ideal candidates for load-bearing structural members that aim to reduce weight and take into account strength. It has become an important development direction of high strength and light metal structure materials used in aerospace. For a newly designed β-titanium alloy, the relationship between microstructure and mechanical properties during aging heat treatment is not clear and need to study further. In this paper, a high-strength β-titanium alloy, Ti-6Mo-5V-3Al-2Fe (wt%), that was designed based on molybdenum equivalent and d-electron theory was investigated. Using vacuum consumable electrode smelting technology, the ingot is obtained by secondary smelting. The transformation point of the alloy is 810 ℃ through calculation and differential thermal analysis. Before aging heat treatment, the solution heat treatment at β field was performance at 850 ℃ for 0.5 h followed by water cooling. The temperature of solution treatment was determined according to the transformation point. In order to study the effect of aging temperatures on microstructure and mechanical properties, various aging temperatures was selected in the range of 400-600 ℃. The aging time is 8 h for all. The effect of aging temperature on the microstructure and tensile properties of the hot-rolled alloy was studied by optical microscope, SEM, TEM, TEM and tensile tester. The microstructure of the alloy after solution heat treatment is mainly consisted by equiaxed β grains and a small part of primary α phase. The solution state alloy has tensile strength R_m=939.5 MPa, a yield strength $R_{p0.2}$=856.7 MPa and elongation A=12.0%. The fracture morphology of the alloy delivers a large number of equiaxed dimples, attributing to the microporous polymeric ductile fracture. After aging treatment with different temperatures, secondary α phases possess different amounts and shapes. In general, the precipitation of secondary phase has significant strengthening effect on the alloy. The ω phase has formed when aged at 400 ℃. The strength of the alloy has little changed while elongation has decreased in this aging temperature. The strength of the alloy was improved significantly due to precipitation of fine secondary α phase when aged at 500 ℃. As the increase of aging temperature, secondary phase gradually grew up and the strength of alloy decreased. The aging temperature has a great influence on the tensile properties of the alloy, which exhibits excellent strength at aging temperature of 500 ℃ and good plasticity at 600 ℃. When the aging temperature is 500 ℃, the optimal match of strength and ductility of the alloy is obtained, which the tensile strength is 1426.52 MPa, yield strength is 1311.34 MPa and elongation is 8.0%.

Keywords: β-titanium alloy, hot rolling, heat treatment, microstructure, mechanical property

Influence of EDTA on the hydroxyapatite coating

Daihua He, Ping Liu, Xinkuan Liu, Xiaohong Chen, Wei Li, Ke Zhang, Fengcang Ma
(School of Materials Science and Engineering, University of Shanghai for Science and Technology)
hedh21@163.com

Abstract: Titanium alloys are becoming the best biomedical implant material due to their low density, low elastic modulus and high corrosion resistance characteristics. The surface modification to improve their bioactivity and biocompatibility has attracted much attention. The bone implant material of titanium alloy with hydroxyapatite (HA) coating, combination the characteristics both of titanium alloy with good mechanical properties and synthetic hydroxyapatite with excellent bioactivity and biocompatibility. The hydrothermal-electrochemical methods is developed on the basis of electrochemical deposition and hydrothermal method. A series of researches were done by our group about the HA coating deposited by hydrothermal chemical method on titanium alloy substrate surface. However, the uniformity and compactness of the coating should be further improved. Ethylenediamine tetraacetic acid disodium (EDTA) is a good chelating agent, which has a wide range of coordination properties and can form stable chelates with almost all metal ions. In the present paper, EDTA was added into the electrolyte. The effects of the EDTA on the HA coating deposited by hydrothermal-electrochemical methods was studied, including the compositions, microstructure, crystallinity, thickness, bonding strength between the coating and structure and biological activity in vitro.

A stainless-steel-autoclave with a teflon liner was used to carry out the experiments of hydrothermal electrochemical deposition. The electrolyte contained 0.025 M $Ca(NO_3)_2$ $4H_2O$, 0.015 M $NH_4H_2PO_4$, 0.1 M $NaNO_3$, and EDTA solution with 0, 2.5×10^{-4}, 5×10^{-4}, 7.5×10^{-4} and 1×10^{-3} M. The pH value of the electrolyte was adjusted to 4.5. The cathode and anode were the Ti_6Al_4V plate and a platinum plate. The electrolyte temperature, the deposition time, the current density values, and the speed of the stirrer were 120 ℃, 120 min. 1.25 mA/cm^2 at galvanostat and 100 r/min, respectively. The results indicate that HA coating is obtained irrespective of whether EDTA was added or not, it has high degree of crystallinity and good biocompatibility. The difference is that the crystal morphology of HA after deposition of EDTA is greatly changed. With the increase of EDTA concentration, HA crystal morphology changed from long flake to petal-like and fibrous band. By increasing the EDTA concentration, the orientation index of the (002) plane of HA decreased, thickness of HA coating decreased too. Bonding strength of HA coatings increase first, and then decrease with increasing the EDTA concentration, reaching the maximum value 16.8 MPa when the concentration is 7.5×10^{-4} M.

Keywords: hydroxyapatite coating, EDTA

Effect of process parameters on the morphology of CNTs/Cu composite powders by water-assisted chemical vapor deposition

Honglei Zhou, Ping Liu, Xiaohong Chen, Wei Li, Liming Bi, Xinkuan Liu
(University of Shanghai for Science and Technology)
zhouyutian007@163.com, Liup516@163.com

Abstract: To solve the problem that the catalysts in the preparation of CNTs/Cu composites are easily dissolved in the matrix and affect the properties of the materials, for the first time, nano-Cr particles precipitated on the surface of Cu-Cr particles are used as catalysts to synthesize CNTs/Cu composite powder in situ by water-assisted chemical vapor deposition (CVD). The morphologies and structures of the samples were characterized by SEM, TEM and Raman spectroscopy. The results show that the Cu-Cr alloy powders have different solution and aging treatment, and the morphology of the nano-Cr particles precipitated on the surface is significantly different. The morphology, length, and diameter of the CNTs synthesized by the catalyst are very different. Among them, the catalysts prepared at 850 ℃ for 60 min solution treatment and at 450 ℃ for 120 min aging treatment had the best morphology, and the wettability of the synthesized CNTs and the matrix Cu particles was good. When the growth temperature is too low, only a small amount of carbon nanotubes are synthesized. As the growth temperature increases, the number of synthesized carbon nanotubes increases and the aspect ratio increases. However, when the growth temperature exceeds 800 ℃, the carbon nanotube wall is rough and the carbon deposition increases. There are a large number of defects, and the quality of carbon nanotubes deteriorates. When the growth temperature is 800 ℃, a large number of carbon nanotubes are synthesized. The tube diameter is mostly in the range of 25-35 nm and the length is 3-5 μm, the surface is relatively smooth; when the growth time is 15 minutes, only a few carbon nanotubes with a very short length and a very small aspect ratio are generated. As the growth time increases, the number of carbon nanotubes produced gradually increases and the length becomes longer. When the reaction time is 60 minutes, the carbon nanotubes grow lushly and the diameter of the tube is uniform, and the aspect ratio can reach 150500. When the reaction time exceeds 60 min, the surface defects of carbon nanotubes increase and the quality of carbon nanotubes deteriorates. When the flow rate of C_2H_4 is 100 mL/min, the number of carbon nanotubes produced is the largest and the quality of carbon nanotubes is the best. When the flow rate of C_2H_4 is lower than 100 mL/min, the number of carbon nanotubes produced is small and the length is short. When the flow rate of C_2H_4 is higher than 100 mL/min, the surface of the carbon nanotubes is coated with different degrees of carbon deposition and carbon nanotubes have many defects. H_2 can promote the growth of carbon nanotubes. When H_2 is not available in the reaction process, the generation of carbon nanotubes can hardly be seen. When the flow rate of H_2 is 2450 mL/min, the quality of the carbon nanotubes produced is best. The water content in the reaction gas is different, and the length, diameter, yield, and purity of the grown carbon nanotubes are different. The water content of 0.4% is most suitable for the growth of carbon nanotubes, resulting in high purity and smooth and clean walls. With a diameter of 20-30 nm and a length of 1800 nm, there is no defect CNTs. The yield of CNTs reached 138%, which was 119% higher than that when the water content was 0, which laid the foundation for the preparation of high-performance CNTs/Cu composites.

Keywords: chemical vapor deposition, CNTs/Cu composite powder, yield, growth temperature, growth time

Effect of ball milling time on properties of Cu/CNTs composites

Shaoli Fu, Ping Liu, Xiaohong Chen
(University of Shanghai for Science and Technology)
15921086537@163.com

Abstract: Firstly, well-distributed Cu/CNTs composite powders were developed by chemical vapor deposition method (CVD) using 10wt%Cr catalyst at a growth temperature of 800 ℃, a growth time of 30 min, and under a mixed $Ar/H_2/C_2H_4$ gas with a flow rate of 800, 2450 and 300 sccm, respectively. The crystal phase and micro morphologies of the composite materials are characterized by scanning electron microscopy (SEM). Then Cu/CNTs mixed powders were obtained by mixing Cu/CNTs composite powders and pure copper powders using high-energy ball milling method. From the SEM images of Cu/CNTs mixed powders, we can conclude that when the milling time was 15 min, the CNTs and pure copper powders in the Cu/CNTs mixed powders were not mixed uniformly, and some Cu/CNTs composite powders are still presenting in the mixed powders as powdery lumps; when the milling time increased to 30 min, the CNTs were almost evenly distributed in the pure copper powder to form uniform Cu/CNTs mixed powders. When the milling time was 45 min, the flake copper powders were deformed and the particle size became smaller under the strong impact of zirconium balls. When the milling time reached to 60 min, the particle size of copper particles were decreasing further, and the integrity of CNTs were destroyed and the aspect ratio of CNTs rapidly decreased. Cu/CNTs composite materials were obtained by spark plasma sintering, and the sintering temperature is 650 ℃, sintering pressure is 35 MPa, the sintering time is 10min, heating rate is 80 ℃/min. The density of the materials was measured by the Archimedes principle. Using the digital metal conductivity tester to measure the conductivity of the composite materials. The micro-tensile tester was used to test the tensile strength of the composite materials. With the increasing of ball milling time, the relative density of composites gradually increased, and the tensile strength and electrical conductivity increased first and then decreased. When the milling time was 45 min, the tensile strength and electrical conductivity reached the maximum, they are 290 MPa and 73%IACS, respectively. From the tensile fractography of the composite materials, we can see that the CNTs are uniformly distributed in the copper matrix, the one end of the CNTs is buried in the grain boundary of the copper matrix, and the other end is wrapped on the surface of the copper crystal grain. Space net structure was formed between the CNTs and the copper grains. The structure can effectively prevent dislocation movement and pin the grain boundary, inhibiting copper grains to grow, so the electrical conductivity and mechanical properties of the composites were improved.

Keywords: milling time, Cu/CNTs mixed powders, Cu/CNTs composite materials, properties

The effect of Ca^{2+} addition on the corrosion resistance of vanadate conversion coating formed on Mg-3Al-3Zn-0.2RE alloy

Fan Zhou, Genshu Zhou
(Xi'an Jiaotong University)
zhougs@mail.xjtu.edu.cn

Abstract: As the lightest metal structural material in current application, magnesium alloys are extensively used in the automobile, aerospace industries and electronic industries. However, due to the high chemical activity and the formation of loose oxide film on the surface, the applications of magnesium alloys are faced with the problem of easy corrosion. Surface modification is thus essential for Mg alloys to improve the corrosion resistance. Among many surface treatment techniques, chemical conversion treatment is an easy and cheap way to achieve surface protection on the magnesium alloys. As an environmentally friendly chemical conversion treatment, the newly developed vanadate conversion coating is a strong candidate to replace traditional chromate conversion coating. But the corrosion resistance of vanadate conversion coatings on magnesium alloys still remains to be improved.

In this study, vanadate conversion coating was prepared on Mg-3Al-3Zn-0.2RE alloy by immersed in vanadium containing bath with Ca^{2+} as an additive. Self-designed Mg-3Al-3Zn0.2RE alloy was casted by vacuum induction melting. Prior to conversion coating, the process operations included alkaline cleaning and acid cleaning. $Ca(NO_3)_2$ was as an additive added to the vanadium conversion bath including $NaVO_3$ (30 g/L) and Na_2WO_4 (10 g/L). The immersion time was 20 minutes and the bath temperature was 90 °. After conversion coating treatment, the specimen was rinsed in deionized water.

The microstructure and constitution of the Mg-3Al-3Zn-0.2RE alloy substrate and the vanadium-based conversion coatings were analyzed by SEM and XPS. The corrosion resistance of the magnesium alloys substrate and the coatings were characterized by potentiodynamic polarization, electrochemical impedance spectroscopy (EIS) and immersion test.

Fig.1 shows the EIS plots of the bare Mg-3Al-3Zn-0.2RE alloy and the vanadium-based conversion coatings with or without Ca^{2+} as an additive on Mg-3Al-3Zn-0.2RE alloy substrates in 3.5%NaCl solution. Compared with the bare Mg-3Al-3Zn-0.2RE alloy, two kind of vanadium-based conversion coatings show better surface resistance, especially the vanadium-based conversion coatings with Ca^{2+} as an additive. By fitting the EIS results with appropriate equivalent circuits, we find that the charge transfer resistance (R_{ct}) of the vanadium-based conversion coating with Ca^{2+} is five times bigger than that of the vanadium-based conversion coating without Ca^{2+}. This result indicates that the addition of Ca^{2+} to vanadium containing bath can improve the corrosion resistance of vanadate conversion coating effectively.

Fig.2 shows the polarization curves of the bare Mg-3Al-3Zn-0.2RE alloy and the vanadium-based conversion coatings with or without Ca^{2+} as an additive on Mg-3Al-3Zn0.2RE alloy substrates in 3.5%NaCl solution. After the formation of vanadate conversion coating, both anodic polarization curve and cathodic polarization curve shift down, indicating the anodic and cathodic reactions are inhibited and the coating effectively enhances the corrosion resistance of the Mg-3Al-3Zn-0.2RE alloy. Although with the addition of Ca^{2+} the corrosion potential of the vanadate conversion coating has a slight decline, the corrosion current density of the vanadate conversion coating obviously reduces. The existence of turning point on the anodic polarization curve of vanadate conversion coatings may be caused by the defects of the coatings.

In summary, the results of the electrochemical measurement demonstrate that the corrosion resistance of Mg-3Al-3Zn-0.2RE alloy is markedly improved by the vanadate conversion treatment with Ca^{2+} as an additive.

Keywords: magnesium alloys,vanadate conversion coating

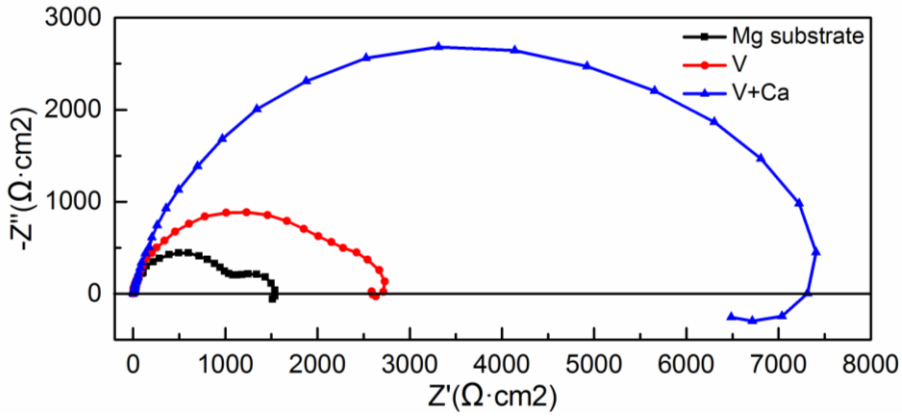

Fig.1 EIS plots of the bare Mg-3Al-3Zn-0.2RE alloy and the vanadium-based conversion coatings with or without Ca^{2+} as an additive on Mg-3Al-3Zn-0.2RE alloy substrates in 3.5%NaCl solution.

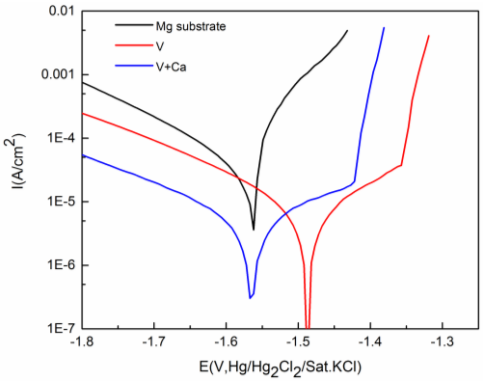

Fig.2 Polarization curves of the bare Mg-3Al-3Zn-0.2RE alloy and the vanadium-based conversion coatings with or without Ca^{2+} as an additive on Mg-3Al-3Zn-0.2RE alloy substrates in 3.5%NaCl solution

Effects of cerium on thermal deformation characteristics of Cu-0.8Mg alloy

Guoqiang Sun, Yong Liu
(School of Materials Science and Engineering, Henan University of Science and Technology)
liuyong@haust.edu.cn

Abstract: With regard to Cu-Mg alloys for high-speed railway contact wires, scholars at home and abroad have conducted some research, but most of the related studies have maintained at around 0.4% of the Mg content, and special processing methods have been adopted to take into account the high strength and high conductivity of copper alloys. But these methods are still a certain distance from the commercial production, with the continuous increase in the speed of high-speed rail, the performance of the contact line material also has more stringent requirements. However, there is relatively little research on thermal deformation of copper alloy with high Mg content at home and abroad. In this erperiment, The Cu-0.8Mg and Cu-0.8Mg-0.15Ce alloys were prepared by smelting in a ZG0.01-40-4 vacuum furnace. The isothermal hot compression test of Cu-0.8Mg and Cu0.8Mg-0.15Ce were carried out on the Gleeble-1500D thermal simulator at the strain temperature range of 500, 600, 700, 800, 850 ℃. and the strain rate range of 0.001, 0.01, 0.1, 1, 10 s^{-1}. the mechanical behavior of Cu-0.8Mg and Cu-0.8Mg-0.15Ce alloy was studied. The relationship between flow stress, the strain temperature and the strain rate was established by thermal physical simulation. And the relationship between flow stress, strain rate and strain temperature of the alloys under different test conditions was studied. The activation energy of hot deformation of Cu-0.8Mg and Cu-0.8Mg-0.15Ce alloys in the process of the isothermal hot compression was calculated. On this basis, the constitutive equation of alloys are constructed, and the hot processing maps of Cu-0.8Mg and Cu-0.8Mg-0.15Ce alloys during hot deformation are obtained by analyzing the hot processing diagram of alloys, thus providing data reference for the formulation of related production processes. The results show that the flow stress curves of the two alloys show typical work hardening, dynamic recovery and dynamic recrystallization characteristics during the hot deformation process. With the increase of deformation temperature and the decrease of the deformation rate, the flow stress and peak stress also decrease, The activation energy of hot deformation of Cu-0.8Mg alloy is 177.88 kJ/mol, and the activation energy of hot deformation of Cu-0.8Mg-0.15Ce alloy is 281.47 kJ/mol, Compared with Cu-0.8Mg.alloy, the addition of Ce increased the activation energy of the alloy by 58%; The hot deformation optimal processing parameters of Cu-0.8Mg alloy during hot deformation could be attained that the deformation temperature was 700-800 ℃ and the strain rate was 0.01-0.1 s^{-1}, The hot deformation optimal processing parameters of 0.8Mg-0.15Ce alloy during hot deformation could also be attained that the strain temperature was 800-850 ℃ and the strain rate was 0.001-0.1 s^{-1}. Compared with the addition of Ce, the hot working temperature of the alloy increased significantly.

Keywords: Cu-0.8Mg alloy, Cu-0.8Mg-0.15Ce alloy, hot deformation, flow stress, hot processing map

The corrosion characteristics of new Cu-7Ni-7Al alloy in artificial seawater

Zhengcheng Song, Shuguo Jia
(Henan University of Science and Technology)
sgjia@haust.edu.cn

Abstract: The corrosion properties of the new Cu-7Ni-7Al alloy in artificial sea water were investigated in this paper. The weight loss and the average corrosion rate of the alloy in artificial seawater were tested by static full immersion test. The electrochemical characteristics of the alloy was illustrated by electrochemical impedance spectroscopy (EIS) and dynamic polarization tests in this work. The static full immersion test demonstrated that the average corrosion rate of the Cu-7Ni-7Al alloy in artificial seawater decreases rapidly from 0.0782 g m^{-2} h^{-1} to 0.0253 g m^{-2} h^{-1} before 144 h. After 144 h, the average corrosion rate tends to be stable and reach the bottom when the time is 240 h. The surface morphology of alloys exposure (remove corrosion products) in artificial sea water for different time was studied by SEM, which have shown significant differences: with the immersion time increasing, the shape of the protective film on the surface of the alloy changes. The protective film changes from loose to compact when the time increases from 24 h to 144 h, it means that the protective effect was improved, which is the main reason for the decreasing of corrosion rate. The state of the protective film is similar when the immersion time is 144 h and 240 h, which means that the surface film of the alloy reaches a stable state after 144 h and the reason of which is the corrosion rate of the alloy tends to be stable. The change of the surface film is a good explanation for the change of corrosion rate, but the appearance of the alloy pitting is also noted. With the increase of immersion time, the pitting phenomenon is more obvious. The more serious pitting grow, the worse corrosion resistance have. The radius of EIS increases faster before 144 h and increases slowly after 144 h. The change of the radius of EIS represents the growth state of oxide film. The trend of surface oxide film can be deduced from the change trend of EIS, which is in accordance with the test results of the corrosion rate. In order to further study the characteristics of the protective film, the equivalent circuit was fitted. it is clear that the corrosion process of the new Cu-Ni-Al alloy in artificial seawater is mainly controlled by the charge transfer resistance R_{ct}. The film resistance Rf and charge transfer resistance R_{ct} increases with time increasing, R_f increases from 25.75 $\Omega \cdot cm^2$ to 58.01 $\Omega \cdot cm^2$, R_{ct} increases from 3.03×10^4 $\Omega \cdot cm^2$ to 9.78×10^4 $\Omega \cdot cm^2$. The dynamic polarization tests show that the polarization curves have similar characteristics, which maybe indicate that the corrosion mechanism of the alloy is consistent. The corrosion potential slightly positive, indicating that the corrosion tendency of the alloy decreases. The current density decreases with the increase of immersion time, the current density is decrease rapidly before 144 h, from 12.86 μA/cm^2 to 4.12 μA/cm^2, and tends to be stable after 144 h, which is correspond with the decrease trend of corrosion rate. Electrochemical tests show that the alloy has good electrochemical characteristics in sea water.

Keywords: Cu-Ni-Al alloy, corrosion rate, polarization curve, electrochemical impedance spectroscopy

Microstructure and properties of MWCNTs/TiB_2 reinforced copper matrix composites fabricated by spark plasma sintering technique

Fei Long[1], Shuguo Jia[1], Xiuhua Guo[1], Kexing Song[1], Shuhua Liang[2], Jiang Feng[2], Shengli Zhang[3], Guohui Li[3]

(1. Key Laboratory of Materials Science and Processing Technology for Non-ferrous Metals of Henan, School of Materials Science and Engineering, Henan University of Science and Technology;
2. School of Materials Science and Engineering, Xi'an University of Technology, China;
3. School of Materials Science and Engineering, Henan University of Science and Technology, China)
sgjia@haust.edu.cn

Abstract: With high electrical and thermal conductivity, and excellent arc erosion resistance, highperformance copper matrix composites possess vast broad prospects in the fields of different low voltage switch such as relays, contactors, circuit breakers and switches. The represent methods used to enhance arc erosion resistance of copper usually decrease its electrical conductivity and thermal conductivity, so there should be a trade-off between arc erosion resistance and the conductivity. In order to improve arc erosion resistance of copper, the ceramic particles TiB_2 with high hardness, high melting point, good thermal conductivity and the lowest resistivity among hard ceramic materials had been chosen to add to copper. In the meantime, the multiwalled carbon nanotubes (MWCNTs) which are one of the most promising one-dimensional nanomaterials in the field of advanced composites due to their extraordinary mechanical, electrical and thermal properties were used as ideal enhancement phase in copper. In order to disperse the MWCNTs in the solution, an anionic dispersants of sodium dodecyl benzene sulfonate (NaDDBS), another anionic dispersants of sodium dodecyl sulfate (SDS) and a nonionic surfactant triton X-100 were used in low concentration of ethanol. The MWCNTs which went through acid treatment and etching, ultrasonic dispersion in mixed dispersants, sensitization and activation were conducted with electroless copper deposition on their surface, eventually. The morphologies of the copper-coated MWCNTs was investigated by field emission scanning electron microscope and X-ray diffraction analysis. Based on electroless deposition technique of the MWCNTs, the copper matrix composites with hybrid reinforcements in different volume ratio were fabricated by spark plasma sintering technique. The relative density, Brinell hardness, electrical conductivity of the developed hybrid copper matrix composites were determined by Archimedes method, Brinell hardness analyzer and an eddy electrical conductivity gage, respectively. Arc erosion behaviors of the copper matrix composites were investigated by electrical contact material testing system. The surface morphologies of the hybrid copper matrix composites after arc erosion were characterized by field emission scanning electron microscope and energy dispersive spectrometer, and the arc duration, mass loss before and after arc erosion were determined simultaneously. The results show that with the total volume fraction of the hybrid reinforcement kept unchanged, the Brinell hardness and electrical conductivity of hybrid copper matrix composites are decreasing as the volume fraction of MWCNTs increases. When the volume fraction of TiB_2 is 6% and the volume fraction of MWCNTs is 0%, the Brinell hardness and electrical conductivity of the hybrid copper matrix composites reach the maximum, respectively. The Brinell hardness and electrical conductivity of hybrid copper matrix composites are 54 HB and 80.73%IACS. In the same total volume fraction, compared with pure copper, the electrical conductivity of hybrid copper matrix composites declined with the increasing the volume ratio of MWCNTs. The effect of MWCNTs on the electrical conductivity of the hybrid copper matrix composites is more than that of TiB_2 particles. Furthermore, the Brinell hardness of the hybrid copper matrix composites increases with the increase in the proportion of TiB_2 volume. The increase of the Brinell hardness of the hybrid copper matrix composites by TiB_2 is more than that of MWCNTs. With the increase in the proportion of TiB_2 volume, the hybrid copper matrix composites present shallower arc erosion pits, less mass loss, and shorter arc duration.

Keywords: spark plasma sintering, copper matrix composites, hybrid reinforcements, Brinell hardness, electrical conductivity, arc erosion behaviors

Copper matrix composites reinforced with mixed size TiB_2 particles

Shengli Zhang[1], Xiuhua Guo[1], Kexing Song[1], Yihui Jiang[2], Fei Long[1], Jiang Feng[1]
(1. Henan University of Science and Technology; 2. Xian University of Technology)
guoxiuhua@sina.com

Abstract: Copper matrix composites reinforced with single size and mixed size TiB_2 particles were prepared by powder metallurgy, investigation has been carried out on effect of mixed size reinforcing particles on the relative density, electrical conductivity, hardness and wear with electrical current properties of the composites. The average particles size of the copper powders used in the test material is 75 μm, TiB_2 particles with average size of 2, 10 and 50 μm are selected as reinforcement materials. Mixing TiB_2 particles with combinations of 2+10 μm, 2+50 μm, 10+50 μm , and the mass ratio of them are both 1:1, 1:2 and 2:1, and then mixed with copper powders, the total volume of TiB_2 particles in the composite is 5%, the preparation of TiB_2/Cu composites material by cold isostatic pressing and vacuum sintering. It is found that when the mass ratio of them are both 1:1, the relative density of the copper matrix composites prepared by the TiB_2 particles combinations of 2 μm and 50 μm can reach 97.9%, and the electrical conductivity or hardness are also higher than those of copper matrix composites reinforced with particles size combinations of 2+10 μm or 10+50 μm. And then compared the mixed size particles combinations of 2 μm and 50 μm with different ratio on properties of copper matrix composites. The results show that the optimal mixing ratio of 2 μm against 50 μm appears to be 1:2, its relative density of 98.5%, hardness of 69 HB and conductivity of 85.3%IACS. Compared to the TiB2/Cu composites reinforced with 2 μm single size particles, the hardness and conductivity of the composites reinforced with mixed size particles can be improved by 12.2% or 4.8% respectively, and compared to the composites reinforced with 50 μm single size particles, its hardness and conductivity can be improved by 9.5% or 3.4% respectively, and compared with the pure copper, its conductivity are decreases by 10.2%, the hardness can be improved by 38%. The current-carrying friction and wear test was carried out when the current of 25 A, load of 0.63 MPa, and speed of 10 m/s. The TiB_2/Cu composites prepared by the combinations of particles size of 2 μm and 50 μm, and them mass ratio are both 1:2, the friction coefficient and wear rate are all decreased compared to the pure copper or composites reinforced with single size particles. TiB_2/Cu composites reinforced with TiB_2 particles with mixed size of 2 μm and 50 μm , the internal defects of 1:2 are less than single size particles as well as the mixed size particles ratio by 1:1 or 2:1. When them ratio are 1:2 the particles distribution are more homogenous, and there is no aggregation or segregation inside. The good enhancement of TiB_2/Cu composites with the mixed size particles is due to the obtained uniform and dense microstructure, the TiB_2 particles with different size particles are more dispersed in the copper matrix, which makes the mixed size particles more synergistic to enhance the copper matrix, which is beneficial to improve the comprehensive properties of the composites.

Keywords: TiB_2/Cu composites, mixed size particles, relative density, microstructure, wear with electrical current

Microstructure analysis (transmission electron microscope) of Ti80 alloy with equiaxed structure

Sijia Quan[1], Kexing Song[1,2], Yanmin Zhang[1,2], Yan Li[1,2], Baojiang Guo[1], Binbin Zhang[3]
(1. Institute of Materials and Engineering, Henan University of Science and Technology, Luoyang, China;
2. Henan Key Laboratory of Advanced Non-ferrous Metals, Luoyang, China;
3. Luoyang Ship Material Research Institute, Luoyang, China)

Abstract: In this paper, the microstructure observation and phase analysis of Ti80 alloy after treated at 900 ℃ for 1 h was studied by means of metallographic microscope and transmission electron microscope, in order to provide theoretical guidance for heat treatment of Ti80 titanium alloy. The results show that the alloy forms equiaxed structure when treated at 900 ℃ for 1 h (the temperature is 100 degrees lower than the $\beta\rightarrow\alpha$ phase transition point) and cooled in the air after the heat preservation. Equiaxial α phase with hexagonal close packed crystal structure (a=0.295 nm; c=0.468 nm) exists in the alloy as a matrix, and there are few internal defects in this phase. A small amount of β phase distributes in the boundary of α phase, which crystal structure is body centered cubic (a=0.328 nm), and there are more internal defects in β phase than in α phase. In addition, visible interface phases with the structure of dislocation layer about 200 nm or parallel-plate around 800 nm can be found between α phase and β phase. The analysis of electron diffraction shows that the interface includes α' phase with close packed hexagonal crystal structure (a=0.308 nm; c=0.470 nm) and F phase with face centered cubic (a=0.426 nm). Among them, α' phase is a kind of transient phase in the $\beta\rightarrow\alpha$ phase transition process during the cooling procedure, which can slightly improves the hardness of the alloy when it exists in the alloy. In this experiment, α' phase exists in equiaxed structure with needle-like microstructure or bar-like tissues, which has high density dislocations inside. Furthermore, the F phase also belongs to the interface phase, which can be formed during the process of β phase change into α phase when the temperature decreases. But the bad thing is that F phase usually exists in titanium alloy as the starting position of dehiscence. In this work, F phase usually exists in the alloy structure with the form of crystal twin. At the same time, according to the results of electron diffraction pattern, it can be observed that diffraction spots of F phase are elongated. So, the judgment can be made that internal layer defects may be emerged in F phase, in addition to the generation of twin crystal inside. The structure in triple junctions of α phase is more complex than other areas, including the structures with the kinds of parallel crates, lumps or needles, and so on. There are a large number of crystal defects in this area, such as high density dislocations, dislocation cells, twin crystal, stacking faults, and so forth. This area consists of three phases by the calibration of electron diffraction, embracing β phase, α' phase and F phase. The three types of phases that existed between α phase grain boundary phase have certain orientation relationship with each other: $(110)\beta//(10\bar{1}0)\alpha'//(111)F$; $[\bar{1}11]\beta//[1\bar{2}1\bar{3}]\alpha'//[\bar{1}10]F$. But in this work, it is regrettable that the influence of the complex organization structure on mechanical properties such as strength, toughness, fatigue properties and corrosion resistance of Ti80 alloy needs to be further studied.

Keywords: Ti80 alloy, microstructure analysis, TEM

Effect of aging treatment and hot deformation on microstructure and properties of Cu-1.5%Ni-0.6%Si-0.15%Ce alloy

Zhuan Zhao
(School of Materials Science and Engineering, Henan University of Science and Technology)
3115773040@qq.com

Abstract: Effect of aging treatment and hot deformation on microstructure and properties of Cu1.5%Ni-0.6%Si-0.15%Ce alloy was studied in this paper. The alloy was melted and cast, and then the solid solution treatment was carried out. The effects of aging temperature and time on the microstructure and properties of the alloy were studied with different deformation of Cu-1.5%Ni-0.6%Si-0.15%Ce alloy. The effect of hardness and conductivity of the alloy was discussed. After aging treatment, Cu-Ni alloy can reach high hardness, good corrosion resistance, high conductivity, thermal conductivity and other excellent properties. It can be widely used and improved in actual production.

The flow stress behavior of Cu-Cr-Zr alloy during hot deformation was studied by isothermal compression test by Gleeble-1500D thermal simulation testing machine at the temperature ranges from 650 ℃ to 850 ℃ and at the strain rate from 0.001 s^{-1} to 10 s^{-1} under the maximum strain of 50%. The dynamic recrystallization microstructure of Cu1.5%Ni-0.6%Si-0.15%Ce alloy was observed under different deformation temperature and different strain rate, microstructure revolution of the Cu-1.5%Ni-0.6%Si-0.15%Ce alloy was observed.

The results show that deformation temperature and strain rate have great influence on the rheological stress of Cu-1.5%Ni-0.6%Si-0.15%Ce alloy. The rheological stress of the Cu1.5%Ni-0.6%Si-0.15%Ce alloy decreases with the increase of deformation temperature and the decrease of strain rate. It is indicated that under this experimental condition, the Cu-1.5%Ni-0.6%Si-0.15%Ce alloy has a positive strain rate sensitivity. Cu-1.5%Ni-0.6%Si-0.15%Ce alloy deformation temperature at 750- 850 ℃, 0.1-1 s^{-1} strain rate under the condition of dynamic recrystallization is the main softening mechanism. And the microstructure and precipitation phase state of Cu-1.5%Ni-0.6%Si-0.15%Ce alloy were affected by deformation temperature and strain rate, the dynamic recrystallization of the alloy is easy to occur under the higher deformation temperature and the smaller strain rate. The microstructure was also strongly depended on the deformation temperature and strain rate. It also observed the Cu-1.5%Ni-0.6%Si-0.15%Ce alloy under different aging process in hardness and electrical conductivity change rule. The hardness and conductivity of Cu-1.5%Ni-0.6%Si-0.15%Ce alloy can be great effected by deformation temperature. The aging precipitation kinetics was obtained. Addition of rare earth element Ce to Cu-1.5%Ni-0.6%Si alloy not only has the effect of refining grain, purifying the matrix, removing impurities, but also improving the hardness and softening temperature of the alloy. The addition of trace elements can improve the comprehensive properties of the CuNi alloy. So Cu-1.5%Ni-0.6%Si-0.15%Ce alloy has high strength, high conductivity and excellent comprehensive performance.

Keywords: Cu-1.5%Ni-0.6%Si-0.15%Ce alloy, aging treatment, thermal simulation, flow stress

The combination of deep cryogenic treatment with the traditional solution and aging treatment of 7050 aluminum alloy

Kaixuan Gu[1], Kaikai Wang[1], Jianpeng Zheng[1,2], Liubiao Chen[1], Jia Guo[1], Chen Cui[1], Junjie Wang[1,2]
(1. CAS Key Laboratory of Cryogenics, Technical Institute of Physics and Chemistry, Beijing, China;
2. University of Chinese Academy of Sciences, Beijing, China)
wangjunjie@mail.ipc.ac.cn

Abstract: The 7050 aluminum alloy have been extensively used in aerospace and automotive industries due to their superior specific strength. Considering its application as high precision components or large-size complex parts, higher dimensional stability and comprehensive properties are still necessary. Deep cryogenic treatment has been well acknowledged as an effective method to improve the mechanical properties, wear resistance and dimensional stability of steels. Studies also revealed that deep cryogenic treatment could improve the properties of aluminum alloy, titanium alloy and magnesium alloy. However, different process technologies have can achieve to different effect. As for tool steel, deep cryogenic treatment is usually conducted after quenching and prior to tempering in order to relieve retained austensite as completely as possible. The solution and aging treatment are the traditional heat treatment of high strength aluminum alloy, however, study on the combination of deep cryogenic treatment with the solution and aging treatment of aluminum alloy is rare. Therefore, the present work is dedicated to investigate the effect of deep cryogenic treatment, which was conducted by combining with the traditional heat treatment on the properties of aluminum alloy.

Deep cryogenic treatment was performed prior to aging and after aging, respectively. The microhardness, tensile properties and fracture toughness of specimens treated by different processes were tested. In order to reveal the effect of deep cryogenic treatment on the aging behavior, the dilatometer experiment was carried out on a Bähr D805L quenching device using 4 mm diameter × 10 mm cylindrical specimens to monitor the aging process of different specimen. Methods of X-ray diffraction, optical microscope (OM), scanning electron microscope (SEM), transmission electron microscope (TEM) were adopted to investigate the microstructural variations caused by deep cryogenic treatment. The results showed that deep cryogenic treatment after aging has little influence on the hardness and mechanical properties of 7050 aluminum alloy. However, deep cryogenic treatment after solution and prior to aging treatment improved the hardness and strength of this alloy. The dilatometric curves showed that the specimen shrinked during aging at 120 ℃, as the relative change in length was reduced in Fig.1. The reduction of relative change in length got smaller due to the conduction of deep cryogenic treatment after solution and prior to aging treatment (SCA), which showed that the treatment had some contribution to the precipitation and stress relief. As a result, the dimensional stability of 7050 aluminum alloy was improved by this treatment t. Microstructural detections revealed that deep cryogenic treatment promoted the precipitates of η phase, which resuted from the change of GP zones. It was concluded that at deep cryogenic treatment after solution and prior to aging treatment changed the aging behavior and precipitates of 7050 aluminum alloy, which improved the mechanical properties and dimensional stability of this alloy.

Keywords: deep cryogenic treatment, 7050 aluminum alloy, mechanical properties, microstructure

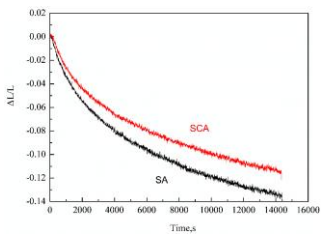

Fig.1 Dilatometric curves under the ageing temperature (120 ℃) of 7050 aluminum alloy after solution (SA) and solution followed with deep cryogenic treatment (SCA)

Effect of cryogenic treatment on titanium Ti-6Al-4V

Yichen Meng, Matteo Villa, Thomas Christiansen, Marcel Somers
(DTU)
tch@mek.dtu.dk, somers@mek.dtu.dk

Abstract: There is increasing focus on the use of titanium and its alloys for applications that require a combination of outstanding corrosion resistance and high mechanical strength. The properties of titanium and its alloys are dictated by the microstructure of the material, which can be "tailored" by heat treatment. Microstructure optimization in titanium and titanium alloys has been the topic of extensive research. However, certain aspects of the heat treatment of titanium alloys, such as the effect of introducing a thermal step at cryogenic temperatures in the thermal cycle, have hitherto been neglected. In the present work the cryogenic behavior of titanium Ti-6Al-4V (Grade 5) is investigated. To this end, Grade 5 Ti was subjected to a systematic set of different heat treatments, including immersion of the material in boiling nitrogen and storage at boiling nitrogen temperature for various times. The material was characterized by optical microscopy, hardness measurement and synchrotron X-Ray diffraction (XRD).

In a first set of experiments, the material was (intercritically) annealed at temperatures in the range 1000-1250 K with intervals of 50 K, followed by moderately slow cooling to room temperature at an average rate of approx. 1 K s^{-1}. The annealing step was intended to partition the alloying elements, i.e. α/β formers, thus resulting in structures (α/β partitioning) with various thermal stability. The material microstructure consisted in various fractions of primary α grains and areas of lamellar α/β microstructure. The fraction of retained β was the largest at the highest applied annealing temperature, i.e. 1250 K. Cryogenic treatment followed and consisted in immersion of the material in boiling nitrogen for various times. Samples where then characterized taking the conventionally treated material as reference. Data show that cryogenic treatment has no direct measurable influence on the material microstructure and hardness.

In a second set of experiments, selected samples, the ones annealed at 1200 and 1250 K, were re-heated to the same temperature applied during annealing, followed by immediate quenching in water. This thermal cycle was meant to produce a martensitic microstructure with 1) varying composition due the partitioning resulting from different annealing temperature, i.e. 1200 K vs 1250 K, and 2) varying the fraction of martensite relative to primary α. Cryogenic treatment was performed afterwards. The microstructure of the material showed a negligible content of β<2%. Data indicate no direct effect of cryogenic treatment on the material microstructure as well as hardness.

In a last set of experiments, conventionally treated as well as cryogenically treated samples were subjected to precipitation hardening treatments at various temperatures. The effect of cryogenic treatment on the material microstructure and the role of composition of the martensite, primary α and β are elucidated.

Keywords: titanium alloy, Ti-6Al-4V, heat treatment, phase transformation, cryogenic treatment

Enrichment behavior of manganese contaminants in continuous annealing process of low carbon steel

Zhideng Wang, Hailing Mu, Weixing Lu, Wen Li
(Meishan Technology Center of Baosteel Central Research Institute)
630376@baosteel.com

Abstract: The requirements of high surface cleanliness of low carbon steel are the inevitable trend of product development in the future. Most of the foreign impurities can be eliminated by conventional cleaning methods, but not include manganese contaminants. It usually have been found in the quenching cell and annealing furnace, which can be transported to the steel surface and form defects. The results of XRD and XRF semi-quantitative analysis indicated that manganese contaminants of precipitates of quench tank have 39.3wt% Mn_3O_4 and 40wt% organic compounds together, and other residues have form of Ca, Mg, Si, Al and P oxides or salts. The collected surface adhesion ash of annealed steel have the chemical content of about 5% Mn and 95% Fe by ICP. The GDS depth analysis of annealed steel show that the steel surface have the behavior of Mn segregation, which its depth is 5 nm depth and maximum value is about 3.2%. Moreover, the special stain defects of steel surface have been studied using SEM-EDS. The results show that Mn content is about 23% well coincided with the results of precipitates of quench tank. Thus, it can be concluded that Mn segregation is the main motive force of enrichment behavior of manganese contaminants. The enrichment behavior can be explained as follows: 1) Mn behavior of precipitation in the grain boundary have been occurred in deformation of induced ferrite and recrystallization mechanism of ferrite in the annealing process; 2) a layer of iron and manganese oxide film have been formed on the surface of steel plate due to Mn segregation and selective oxidation with the micro oxygen in the reductive atmosphere; 3) the oxide film is stripped from steel surface by friction of the rolls during operation and transmission, which part translate into furnace ash, and the other part have been brought into the quenching tank as manganese contaminants; 4) the manganese contaminants have been transferred and adhered to steel surface when strip steel through quench tank, and an surface compressional defects formed eventually by leveling process.

Keywords: low carbon steel, continuous annealing process, manganese impurities, enrichment behavior

Hot deformation behavior and aging treatment of Cu-Zr-Y alloy

Xiaohui Zhang, Baohong Tian, Yi Zhang, Kexing Song, Bingjie Wang, Yong Liu
(School of Materials Science and Engineering, Henan University of Science and Technology)
samuel0361@163.com

Abstract: Along with the rapid development of economy and science, electronic information industry has drawn much attention. So the tremendous progress have taken place in the copper alloy industry. The principal properties of ideal lead frame material is that the tensile strength, hardness and electrical conductivity are more than 600 MPa, 180 HV and 80%IACS respectively. Because of the high strength, high electrical conductivity and good heat resistance, the Cu-Zr alloy is the most prospective materials in lead-frame for large scale integrated circuit.

In this paper, The Cu-Zr alloys were cast in a vacuum induction furnace. The rare earth element Y was added to the alloy. The hot deformation behavior of Cu-Zr-Y alloy were studied at a Gleeble-1500D thermal-mechanical simulator in the temperature range of 550-900 ℃ and at the strain rate ranging from 0.001 s^{-1} to 10 s^{-1} under maxium strain of 55%. The relationship of stress-strain curves, alloy structure, recovery and recrystallization were analyzed and discussed. Cold deformation treatment was carried out with different degrees after solid solution treatment at 900 ℃ for one hour, then the Cu-Zr-Y alloy was aging treated at 400-550 ℃, within the range of time from 15 minutes to 6 hours. The effects of cold deformation degree, aging temperature and aging time on the electrical conductivity and microhardness were studied.

It was found that strain rate and deformation temperature changes significantly affected the flow stress level of Cu-Zr-Y alloy, the flow stress and peak stress increases with the decreasing deformation temperature and the increasing strain rate. What is more, the higher the deformation temperature, the more prone alloy dynamic recrystallization can be obtained. With the enhance of aging temperature and the increase of cold deformation. The more second phase precipitated. After aging treatment, the hardness and electrical conductivity is improved, while the alloy after cold deformation, resulting in a high density of dislocations. The reason of Y addition affecting the recovery and recrystallization is that the rare earth atoms have the tendency to assemble at crystal defects and grain boundary, which prevents the dislocations from glide. Through above analysis the hot deformation behavior and dynamic recrystallization theory can be enriched and the practical production process can benefits from this study.

Keywords: Cu-Zr-Y alloy, hot compression, deformation, flow stress, dynamic recrystallization, cold deformation, aging treatment

Effect of thermo-mechanical treatment on microstructure and properties of Cu-Be-Co alloy

Yanjun Zhou[1], Kexing Song[1], Xiuhua Guo[1], Yanmin Zhang[1], Baojiang Guo[2]
(1. Henan University of Science and Technology, Collaborative Innovation Center of Nonferrous Metals;
2. Henan University of Science and Technology)
dazhou456@163.com

Abstract: In this paper, the Cu-0.2Be-0.8Co alloy consisted of 0.23wt% beryllium and 0.84wt% cobalt along with balance of copper was regarding as the object of study. The Cu-0.2Be0.8Co alloy was prepared through thermo-mechanical treatment after subsequent solid solution, cold deformation, and aging. The specimens were solution treated at 950 ℃ for 60 min and then quenched in water, followed by cold deformation with 10%, 20%, 30%, 40%, 50% and 60%, respectively. The aging treatment parameter was at 460 ℃ holding for 240 min and cooled in air. The properties of hardness and electrical conductivity was measured using a HB-3000 hardness tester and Sigma 2008 B/C digital eddy current metal conductivity tester, respectively. The microstructure of Cu-0.2Be-0.8Co alloy after different thermo mechanical treatment was observed by transmission electron microscopy (TEM). The results show that the effect of thermo-mechanical treatment on hardness is more obvious than that of electrical conductivity. After thermo-mechanical treatment, the hardness is significantly improved with the increase of cold deformation, yet the change of electrical conductivity is not obvious. When the cold deformation is 50%, the hardness of Cu-0.2Be0.8Co alloy increases remarkably from 117 HB to 176 HB. The increase rate is reach to 50.4% compared to the hardness value in solution condition. However, the electrical conductivity increases gradually form 71.6%IACS to 72.7%IACS with cold deformation from 0 to 50%, and the increase rate is 1.5%. Microstructure observation shows that the dislocation density increases significantly and the size of the precipitated phase is finer and more diffuse after thermo-mechanical treatment. The precipitation rate of precipitated phase is significantly accelerated after 50% cold deformation, and there are discontinuous precipitation phenomena.

Keywords: Cu-0.2Be-0.8Co alloy, thermo-mechanical treatment, hardness, electrical conductivity, microstructure

Effect of long-period stacking ordered phase on hot tearing susceptibility of Mg-Zn-*x*Y alloys

Ye Zhou, Pingli Mao
(Shenyang University of Technology)
pinglimao@yahoo.com

Abstract: The effect of long-period stacking ordered (LPSO) phase on hot tearing susceptibility (HTS) of Mg-1Zn-*x*Y alloys and the influence of *m*(Zn)/*m*(Y) ratio on Mg-Zn-Y system alloys were investigated experimentally using a home-made T-type hot tearing mould. The characteristic parameters related to HTS during the solidification process were measured by cooling curve thermal analysis. The microstructure and the morphology of crack zone were characterized by scanning electron microscopy (SEM) and electron back scatter diffraction (EBSD), and the composition of alloys was analyzed by X-ray diffraction (XRD). The result showed that LPSO phase formed when *m*(Zn)/*m*(Y)＜1, and the LPSO content increased with increasing of Y. LPSO phase could benefit eutectic refilling and decrease the HTS, and high *m*(Zn)/*m*(Y) ratio exhibited low HTS.

Keywords: Mg-Zn-Y alloys, hot tearing susceptibility, thermal analysis, *m*(Zn)/*m*(Y) ratio

Manufacturing of Al alloy closed cell foams using shell as foaming agent

Junwen Li
(Dalian Jiao-Tong Univercity)
joelee0527@163.com

Abstract: Metallic foams are commonly produced using hydride and carbonates foaming agents. However carbonate foaming agents are safer to handle than hydrides and produce aluminum foam with a fine, homogenous cell structure, low cost and easily available. The number of pores per inch (PPI) and relative density of the foam play an important role on their physical and mechanical properties. Hence it is very important to investigate effect of shell foaming agent on PPI and relative density. The present work deals with the effect of additive amount of the shell forming agent on the physical properties of an AlSi7Mg alloy closed cell foam. The foam was produced with different additive amount of shell (1, 3, 5 wt%) as a foaming agent. The PPI and density of the foam produced with different additive amount of shell as foaming agent are determined. Relative density is in the range of 0.21-0.29, PPI are in the range of 11-19 for the produced AlSi7Mg alloy closed cell foam. Therefore, the appropriate addition amount of shell is 3% by weight for production of a uniform cell structure from the viewpoints of efficiency and economy.

Keywords: aluminum foam, foaming process

Effect of interrupted ageing T8I6 and T9I6 on microstructure and mechanical properties of aluminum alloy 2519A

Daxiang Sun[1], Lingying Ye[2], Yunlai Deng[2], Jianguo Tang[2], Xinming Zhang[2], Xinghui Gui[3], Gang Sha[4]
(1. Guangdong Industrial Analysis and Testing Center;
2. School of Materials Science and Engineering, Central South University;
3. Chinalco Materials Application Research Institute Co., Ltd., Suzhou Branch;
4. School of Materials Science and Engineering, Nanjing University of Science and Technology)

Abstract: The effect of interrupted ageing process T8I6 and T9I6 on the microstructure and mechanical properties of aluminum alloy 2519A was studied by means of hardness, tensile test, TEM (Transmission Electron Microscope) and APT (Atom Probe Tomography). The yield and tensile strength of 2519A-T9I6 alloy were greatly increased, reaching 495 MPa and 530 MPa, compared to 2519A-T8I6, reaching 445 MPa and 483 MPa. After T9I6 treatment, θ′ precipitates in 2519A alloy become finer and denser than those in T8I6 alloy, which makes the strength improve obviously. The APT results show that after pre-deformation and pre-aging, the distribute of the clusters in 2519A-T9I6 is much denser and uniform, while the clusters in 2519A-T8I6 is badly concentrated around the dislocations, which is the main reason for the difference in properties between the two alloys.

Keywords: aluminum alloy 2519A, interrupted ageing, mechanical properties, precipitates, clusters

Effects of anneal temperature on the microstructure and mechanical properties of 7050 alloy during thermal-mechanical treatment process

Linchi Zou[1], Junfeng Chen[2]
(1. Fujian University of Technology; 2. Fuzhou Univertisy)
zoulinchi@fjut.edu.cn

Abstract: During the thermal-mechanical treatment (TMT) process the anneal apparently affects on the microstructure and mechanical properties of aluminum alloy, and it is one key point to regulate microstructure and improve properties. In this paper, the effects of anneal temperature on the microstructure and mechanical properties of 7050 alloy by TMT process was investigated. It is found that the interaction between recovery and precipitation during the anneal process, when 70% deformed specimens annealed in the temperature range of 250-340 ℃. In low temperature anneal process, the precipitation improved by deformed microstructure suppress the recovery and recrystallization behaviour. However, precipitation decays fast and recovery enhances with increasing temperature. In specimens, the deformed microstructure transforms into dislocation cells and sub-grains. When 70% deformed specimens annealed in the temperature range of 370-400 ℃, the recrystallization behaviour is dominant and alloy elements dissolved into matrix, which results in recrystallizated grain instead of deformed microstructure. Besides, the strength of 7050 aluminum alloy ascend firstly then descend with increasing temperature, but the elongation keep rise.

Keywords: 7050 alloy, thermal-mechanical treatment, microstructure, anneal

Effects of low temperature plasma nitriding on the wear and fatigue properties of Ti-6Al-4V alloy

Shouming Yu, Guojun Zhang, Lijing Bai, Shuai Ren, Tao Wang, Yichao Gong
(Xi'an University of Technology)
zhangguojun@xaut.edu.cn

Abstract: A low temperature plasma nitriding treatment was performed at 500 ℃ for 24 h under gas mixture of N_2/Ar=4. This treatment formed a thin compound layer (CL) (2 μm) and a nitrogen diffusion zone (DZ) (~27.5 μm) on the surface of Ti-6Al-4V alloy. In order to evaluate the wear and fatigue properties of the treated Ti-6Al-4V, dry wear and rotation bending fatigue tests were conducted. Compared with untreated Ti-6Al-4V, the low temperature plasma nitrided Ti-6Al-4V exhibited higher wear resistance but inferior fatigue properties. The fatigue failure mechanisms were identified by examination of the fracture surfaces. It was found that fatigue cracks mainly initiated from the CL surface and the CL/DZ interface due to the poor toughness of CL and the mismatch of mechanical properties (e.g. hardness and elasticity modulus) between CL and DZ. More remarkable, when removing the CL by mechanical polishing, the residual DZ could simultaneously improve the wear and fatigue performance of Ti-6Al-4V alloy. The S-N curves were constructed, and the endurance limit of the treated Ti-6Al-4V after removing the CL was raised to 560 MPa which was higher than those obtained by conventional nitriding treatments performed at 600-1100 ℃ reported in literature. This was attributed to the gradient distribution of nitrogen composition followed by gradient changes of mechanical properties in DZ, which reduced the mismatch of mechanical properties between DZ and Ti-6Al-4V substrate.

Keywords: low temperature plasma nitriding, Ti-6Al-4V alloy, wear, fatigue